
Whole-Genome Random Sequencing and Assembly of *Haemophilus Influenzae* Rd
Author(s): Robert D. Fleischmann, Mark D. Adams, Owen White, Rebecca A. Clayton, Ewen F. Kirkness, Anthony R. Kerlavage, Carol J. Bult, Jean-Francois Tomb, Brian A. Dougherty, Joseph M. Merrick, Keith McKenney, Granger Sutton, Will FitzHugh, Chris Fields, Jeannie D. Gocyne, John Scott, Robert Shirley, Li-Ing Liu, Anna Glodek, Jenny M. Kelley, Janice F. Weidman, Cheryl A. Phillips, Tracy Spriggs, Eva Hedblom, Matthew D. Cotton, Teresa R. Utterback...

Source: *Science*, New Series, Vol. 269, No. 5223 (Jul. 28, 1995), pp. 496-498+507-512

Published by: American Association for the Advancement of Science

Stable URL: <https://www.jstor.org/stable/2887657>

Accessed: 31-08-2019 14:35 UTC

JSTOR is a not-for-profit service that helps scholars, researchers, and students discover, use, and build upon a wide range of content in a trusted digital archive. We use information technology and tools to increase productivity and facilitate new forms of scholarship. For more information about JSTOR, please contact support@jstor.org.

Your use of the JSTOR archive indicates your acceptance of the Terms & Conditions of Use, available at <https://about.jstor.org/terms>



JSTOR

American Association for the Advancement of Science is collaborating with JSTOR to digitize, preserve and extend access to *Science*

Whole-Genome Random Sequencing and Assembly of *Haemophilus influenzae* Rd

Robert D. Fleischmann, Mark D. Adams, Owen White, Rebecca A. Clayton, Ewen F. Kirkness, Anthony R. Kerlavage, Carol J. Bult, Jean-Francois Tomb, Brian A. Dougherty, Joseph M. Merrick, Keith McKenney, Granger Sutton, Will FitzHugh, Chris Fields,* Jeannine D. Gocayne, John Scott, Robert Shirley, Li-Ing Liu, Anna Glodek, Jenny M. Kelley, Janice F. Weidman, Cheryl A. Phillips, Tracy Spriggs, Eva Hedblom, Matthew D. Cotton, Teresa R. Utterback, Michael C. Hanna, David T. Nguyen, Deborah M. Saudek, Rhonda C. Brandon, Leah D. Fine, Janice L. Fritchman, Joyce L. Fuhrmann, N. S. M. Geoghagen, Cheryl L. Gnehm, Lisa A. McDonald, Keith V. Small, Claire M. Fraser, Hamilton O. Smith, J. Craig Venter†

An approach for genome analysis based on sequencing and assembly of unselected pieces of DNA from the whole chromosome has been applied to obtain the complete nucleotide sequence (1,830,137 base pairs) of the genome from the bacterium *Haemophilus influenzae* Rd. This approach eliminates the need for initial mapping efforts and is therefore applicable to the vast array of microbial species for which genome maps are unavailable. The *H. influenzae* Rd genome sequence (Genome Sequence DataBase accession number L42023) represents the only complete genome sequence from a free-living organism.

A prerequisite to understanding the complete biology of an organism is the determination of its entire genome sequence. Several viral and organellar genomes have been completely sequenced. Bacteriophage ϕ X174 [5386 base pairs (bp)] was the first to be sequenced, by Fred Sanger and colleagues in 1977 (1). Sanger *et al.* were also the first to use strategy based on random (unselected) pieces of DNA, completing the genome sequence of bacteriophage λ (48,502 bp) with cloned restriction enzyme fragments (1). Subsequently, the 229-kb genome of cytomegalovirus (CMV) (2), the 192-kb genome of vaccinia (3), and the 187-kb mitochondrial and 121-kb chloroplast genomes of *Marchantia polymorpha* (4) have been sequenced. The 186-kb genome of variola (smallpox) was the first to be completely sequenced with automated technology (5).

At the present time, there are active genome projects for many organisms, including *Drosophila melanogaster* (6), *Escherichia coli* (7), *Saccharomyces cerevisiae* (8), *Bacillus subtilis* (9), *Caenorhabditis elegans* (10), and

J.-F. Tomb, B. A. Dougherty, and H. O. Smith are with the Johns Hopkins University School of Medicine, Baltimore, MD 21205, USA. J. M. Merrick is with the State University of New York, Department of Microbiology, Buffalo, NY, 14214, USA. K. McKenney is with the National Institute for Standards and Technology, Gaithersburg, MD 20878, USA. All other authors are with The Institute for Genomic Research (TIGR), Gaithersburg, MD, 20878, USA. The address for TIGR as of 9 September 1995 is 9712 Medical Center Drive, Rockville, MD 20850, USA.

*Present address: The National Center for Genome Resources, Santa Fe, NM, 87505, USA.

†To whom correspondence should be addressed.

Homo sapiens (11). These projects, as well as viral genome sequencing, have been based primarily on the sequencing of clones usually derived from extensively mapped restriction fragments, or λ or cosmid clones. Despite advances in DNA sequencing technology (12) the sequencing of genomes has not progressed beyond clones on the order of the size of λ (~40 kb). This has been primarily because of the lack of sufficient computational approaches that would enable the efficient assembly of a large number (tens of thousands) of independent, random sequences into a single assembly.

The computational methods developed to create assemblies from hundreds of thousands of 300- to 500-bp complementary DNA (cDNA) sequences (13) led us to test the hypothesis that segments of DNA several megabases in size, including entire microbial chromosomes, could be sequenced rapidly, accurately, and cost-effectively by applying a shotgun sequencing strategy to whole genomes. With this strategy, a single random DNA fragment library may be prepared, and the ends of a sufficient number of randomly selected fragments may be sequenced and assembled to produce the complete genome. We chose the free-living organism *Haemophilus influenzae* Rd as a pilot project because its genome size (1.8 Mb) is typical among bacteria, its G+C base composition (38 percent) is close to that of human, and a physical clone map did not exist.

Haemophilus influenzae is a small, nonmotile, Gram-negative bacterium whose only

natural host is human. Six *H. influenzae* serotype strains (a through f) have been identified on the basis of immunologically distinct capsular polysaccharide antigens. Non-typeable strains also exist and are distinguished by their lack of detectable capsular polysaccharide. They are commensal residents of the upper respiratory mucosa of children and adults and cause otitis media and respiratory tract infections, mostly in children. More serious invasive infection is caused almost exclusively by type b strains, with meningitis producing neurological sequelae in up to 50 percent of affected children. A vaccine based on the type b capsular antigen is now available and has dramatically reduced the incidence of the disease in Europe and North America.

Genome sequencing. The strategy for a shotgun approach to whole genome sequencing is outlined in Table 1. The theory follows from the Lander and Waterman (14) application of the equation for the Poisson distribution. The probability that a base is not sequenced is $P_0 = e^{-m}$, where m is the sequence coverage. Thus after 1.83 Mb of sequence has been randomly generated for the *H. influenzae* genome ($m = 1, 1 \times$ coverage), $P_0 = e^{-1} = 0.37$ and approximately 37 percent of the genome is unsequenced. Fivefold coverage (approximately 9500 clones sequenced from both insert ends and an average sequence read length of 460 bp) yields $P_0 = e^{-5} = 0.0067$, or 0.67 percent unsequenced. If L is genome length and n is the number of random sequence segments done, the total gap length is Le^{-m} , and the average gap size is L/n . Fivefold coverage would leave about 128 gaps averaging about 100 bp in size.

To approximate the random model during actual sequencing, procedures for library construction (15) and cloning (16) were developed. Genomic DNA from *H. influenzae* Rd strain KW20 (17) was mechanically sheared, digested with BAL 31 nuclease to produce blunt ends, and size-fractionated by agarose gel electrophoresis. Mechanical shearing maximizes the randomness of the DNA fragments. Fragments between 1.6 and 2.0 kb in size were excised and recovered. This narrow range was chosen to minimize variation in growth of clones. In addition, we chose this maximum size to minimize the number of complete genes that might be present in a single fragment, and thus might be lost as a result of expression of deleterious gene products. These fragments were ligated to Sma I-cut, phosphatase-treated pUC18 vector, and the ligated products were fractionated on an agarose gel. The linear vector plus insert band was excised and recovered. The ends of the linear recombinant molecules were repaired with T4 polymerase, and the molecules were then ligated into circles. This two-

stage procedure resulted in a collection of single-insert plasmid recombinants with minimal contamination from double-insert chimeras (<1 percent) or free vector (<3 percent). Because deviation from randomness is most likely to occur during cloning, *E. coli* host cells deficient in all recombination and restriction functions (18) were used to prevent rearrangements, deletions, and loss of clones by restriction. Transformed cells were plated directly on antibiotic diffusion plates (16) to avoid the usual broth recovery phase that would have allowed multiplication and selection of the most rapidly growing cells and could lead to deviation from randomness. All colonies were used for template preparation regardless of size. Only clones lost because of expression of deleterious gene products would be deleted from the library, resulting in a slight increase in gap number over that expected.

To evaluate the quality of the *H. influenzae* library, sequence data were obtained from ~4000 templates by means of the M13-21 primer. Sequence fragments were assembled with the AUTOASSEMBLER software [Applied Biosystems division of Perkin-Elmer (AB)] after obtaining 1300, 1800, 2500, 3200, and 3800 sequence fragments, and the number of unique assembled base pairs was determined. The data obtained from the assembly of up to 3800 sequence fragments were consistent with a Poisson distribution of fragments with an average "read" length of 460 bp for a genome of 1.9×10^6 bp, indicating that the library was essentially random.

Plasmid DNA templates that were double-stranded and of high quality (19,687) were prepared by a method developed in collaboration with Advanced Genetic Technology Corporation (19). Plasmids were prepared in a 96-well format for all stages of DNA preparation from bacterial growth through final DNA purification. Template concentration was determined with Hoechst dye and a Millipore Cytofluor 2350. DNA concentrations were not adjusted, but low-yielding templates (<30 ng/ μ l) were identified where possible and not sequenced. Templates were also prepared from two *H. influenzae* λ genomic libraries (20). An amplified library was constructed in vector λ GEM-12 and an unamplified library was constructed in λ DASH II. Both libraries contained inserts in the size range of 15 to 20 kb. Liquid lysates (10 ml) were prepared from selected plaques and templates were prepared on an anion-exchange resin (Qiagen). Sequencing reactions were carried out on plasmid templates by means of a Catalyst LabStation (AB) and PRISM Ready Reaction Dye Primer Cycle Sequencing Kits (AB) for the M13 forward (M13-21) and the M13 reverse (M13RP1)

primers (21). Dye terminator sequencing reactions were carried out on the λ templates on a Perkin-Elmer 9600 Thermocycler with the Applied Biosystems Prism Ready Reaction Dye Terminator Cycle Sequencing Kits. We used T7 and SP6 primers to sequence the ends of the inserts from the λ GEM-12 library and T7 and T3 primers to sequence the ends of the inserts from the λ DASH II library. Sequencing reactions (28,643) were performed by eight individuals using an average of 14 AB 373 DNA Sequencers per day over a 3-month period. All sequencing reactions were analyzed with the Stretch modification of the AB 373 sequencer. These sequencers were modified to include a heat plate and the height of the laser was reduced. With standard gel plates the "well-to-read" length was increased to 34 cm when standard sequencing plates were used and to 48 cm when 60-cm plates were used. The sequencing reactions in this project were analyzed primarily with a 34-cm well-to-read distance. The overall sequencing success rate was 84 percent for M13-21 sequences, 83 percent for M13RP1 sequences, and 65 percent for dye-terminator reactions. The average usable read length was 485 bp for M13-21 sequences, 444 bp for M13RP1 sequences, and 375 bp for dye-terminator reactions. The high-throughput sequencing phase of the project is summarized in Table 2.

We balanced the desirability of sequencing templates from both ends, in terms of ordering of contigs and reducing the cost of lower total number of templates, against shorter read lengths for sequencing reactions performed with the M13RP1 primer compared to the M13-21 primer. Approximately one-half of the templates were sequenced from both ends. Altogether, 9297 M13RP1 sequencing reactions were done. Random reverse sequencing reactions were done on the basis of successful forward se-

quencing reactions. Some M13RP1 sequences were obtained in a semidirected fashion; for example, M13-21 sequences pointing outward at the ends of contigs were chosen for M13RP1 sequencing in an effort to specifically order contigs. The semidirected strategy was effective, and clone-based ordering formed an integral part of assembly and gap closure.

In the course of our research on expressed sequence tags (ESTs), we developed a laboratory information management system for a large-scale sequencing laboratory (22). The system was designed to automate data flow wherever possible and to reduce user error. It has at its core a series of databases developed with the Sybase relational data management system. The databases store and correlate all information collected during the entire operation from template preparation to final analysis. Although the system was originally designed for EST projects, many of its features were applicable or easily modified for a genomic sequencing project. Because the raw output of the AB 373 sequencers is collected on a Macintosh system and our data management system is based on a Unix system, it was necessary to design and implement multi-user, client-server applications that allow the raw data as well as analysis results to flow seamlessly into the database with a minimum of user effort. To process data collected by the AB 3735, sequence files were first analyzed with FACTURA, an AB program that runs on the Macintosh and is designed for automatic vector sequence removal and end-trimming of sequence files. The Macintosh program ESP, written at The Institute for Genomic Research (TIGR), loaded the feature data extracted from sequence files by FACTURA to the Unix-based *H. influenzae* relational database. Assembly was accom-

Table 1. Whole-genome sequencing strategy.

Stage	Description
Random small insert and large insert library construction	Shear genomic DNA randomly to ~2 kb and 15 to 20 kb, respectively
Library plating	Verify random nature of library and maximize random selection of small insert and large insert clones for template production
High-throughput DNA sequencing	Sequence sufficient number of sequence fragments from both ends for 6 \times coverage
Assembly	Assemble random sequence fragments and identify repeat regions
Gap closure	
Physical gaps	Order all contigs (fingerprints, peptide links, λ clones, PCR) and provide templates for closure
Sequence gaps	Complete the genome sequence by primer walking
Editing	Inspect the sequence visually and resolve sequence ambiguities, including frameshifts
Annotation	Identify and describe all predicted coding regions (putative identifications, starts and stops, role assignments, operons, regulatory regions)

plished by first retrieving a specified set of sequence files and their associated features by means of STP, another TIGR program, which is an X-windows graphical interface that retrieves sequences from the database with user-defined queries.

TIGR ASSEMBLER is the software component that enabled us to assemble the *H. influenzae* genome. It simultaneously clusters and assembles fragments of the genome. In order to obtain the speed necessary to assemble more than 10⁴ fragments, the algorithm builds a table of all 10-bp oligonucleotide subsequences to generate a list of potential sequence fragment overlaps. When TIGR ASSEMBLER is used, a single fragment begins the initial contig; to extend the contig, a candidate fragment is chosen with the best overlap based on oligonucleotide content. The current contig and candidate fragment are aligned by a modified version of the Smith-Waterman (23) algo-

rithm, which provides for optimal gapped alignments. The contig is extended by the fragment only if strict criteria for the quality of the match are met. The match criteria include the minimum length of overlap, the maximum length of an unmatched end, and the minimum percentage match. The algorithm automatically lowers these criteria in regions of minimal coverage and raises them in regions with a possible repetitive element. The number of potential overlaps for each fragment determines which fragments are likely to fall into repetitive elements. Fragments representing the boundaries of repetitive elements and potentially chimeric fragments are often rejected on the basis of partial mismatches at the needs of alignments and excluded from the contig.

TIGR ASSEMBLER was designed to take advantage of clone size information coupled with sequence information from both ends of each template. It enforces the

constraint that sequence fragments from two ends of the same template point toward one another in the contig and are located within a certain range of base pairs (definable for each clone on the basis of the insert length or the clone size range for a given library). In order for the assembly process to be successful it was essential that the sequence data be of the highest quality and that sequence fragment lengths be sufficient to span most small repeats. Less than 13 percent of our random sequence fragments were smaller than 400 bp after vector removal and end trimming. Assembly of 24,304 sequence fragments of *H. influenzae* required 30 hours of central processing unit time with the use of one processor on a SPARCcenter 2000 containing 512 Mb of RAM. This process resulted in approximately 210 contigs. Because of the high stringency of the TIGR ASSEMBLER, all contigs were searched against each other with GRASTA, which is a modified version of the program FASTA (24). In this way, additional overlaps that enabled compression of the data set into 140 contigs were detected. The location of each fragment in the contigs and extensive information about the consensus sequence itself were loaded into the *H. influenzae* relational database.

After assembly, the relative positions of the 140 contigs were unknown. The program ASM_ALIGN, developed at TIGR, identified clones whose forward and reverse sequencing reactions indicated that they were in different contigs and ordered and displayed these relationships. With this program, the 140 contigs were placed into 42 groups totaling 42 physical gaps (no template DNA for the region) and 98 sequence gaps (template available for gap closure).

Four integrated strategies were developed to order contigs separated by physical gaps. Oligonucleotide primers were designed and synthesized from the end of each contig group. These primers were then available for use in one or more of the strategies outlined below:

1) DNA hybridization (Southern) analysis was done to develop a "fingerprint" for a subset of 72 of the above oligonucleotides. This procedure was based on the supposition that labeled oligonucleotides homologous to the ends of adjacent contigs should hybridize to common DNA restriction fragments, and thus share a similar or identical hybridization pattern or fingerprint (25). Adjacent contigs identified in this manner were targeted for specific PCR reactions.

2) Peptide links were made by searching each contig end with BLASTX (26) against a peptide database. If the ends of two contigs matched the same database sequence appropriately, then the two contigs were tentatively considered to be adjacent.

Table 2. Summary of features of whole-genome sequencing of *H. influenzae* Rd.

Description	Number
Double-stranded templates	19,687
Forward-sequencing reactions (M13-21 primer)	19,346
Successful (%)	16,240 (84)
Average edited read length (bp)	485
Reverse sequencing reactions (M13RP1 primer)	9,297
Successful (%)	7,744 (83)
Average edited read length (bp)	444
Sequence fragments in random assembly	24,304
Total base pairs	11,631,485
Contigs	140
Physical gap closure	42
PCR	37
Southern analysis	15
λ clones	23
Peptide links	2
Terminator sequencing reactions*	3,530
Successful (%)	2,404 (68)
Average edited read length (bp)	375
Genome size (bp)	1,830,137
G+C content (%)	38
rRNA operons	6
rrnA, rrnC, rrnD (spacer region) (bp)	723
rrnB, rrnE, rrnF (spacer region) (bp)	478
tRNA genes identified	54
Number of predicted coding regions	1,743
Unassigned role (%)	736 (42)
No database match	389
Match hypothetical proteins	347
Assigned role (%)	1,007 (58)
Amino acid metabolism	68 (6.8)
Biosynthesis of cofactors, prosthetic groups, and carriers	54 (5.4)
Cell envelope	84 (8.3)
Cellular processes	53 (5.3)
Central intermediary metabolism	30 (3.0)
Energy metabolism	105 (10.4)
Fatty acid and phospholipid metabolism	25 (2.5)
Purines, pyrimidines, nucleosides and nucleotides	53 (5.3)
Regulatory functions	64 (6.3)
Replication	87 (8.6)
Transcription	27 (2.7)
Translation	141 (14.0)
Transport and binding proteins	123 (12.2)
Other	93 (9.2)

*Includes gap closure, walks on rRNA repeats, random end-sequencing of λ clones for assembly confirmation, and alternative reactions for ambiguity resolution.

Hit#	Identification	%Sim	Hit#	Identification	%Sim	Hit#	Identification	%Sim	Hit#	Identification	%Sim
0369	His-tRNA Sase (hisS)	79	0785	ribosomal prt L29 (rpl29)	87	0610	L-fucose permease (fucP)	59	1462	nodulation prt T (nodT)	46
0362	Ile-tRNA Sase (ileS)	78	0777	ribosomal prt L30 (rpl30)	86	1218	L-lactate permease (lctP)	54	0549	rRNA (adenosine-N6,N6-)	81
1211	Lys-tRNA Sase (leuS)	82	0796	ribosomal prt L31 (rpl31)	92	1729	lactam utilization prt (lamB)	60		dimethyltransferase (ksgA)	
0636	Lys-tRNA Sase analog (genX)	84	0758	ribosomal prt L32 (rpl32)	86	0623	methylgalactoside permease ATP-BP (mgIA)	85	0511	tellurite resistance prt (tehA)	62
0623	Met-tRNA formyltransferase (fmt)	77	0158	ribosomal prt L33 (rpl33)	85	01	methylgalactoside-BP (mgIB)	81	1275	tellurite resistance prt (tehB)	71
1276	Met-tRNA Sase (metG)	83	0398	ribosomal prt L34 (rpl34)	93	0824	methylgalactoside permease (mgC)	90		<i>Phage-related functions and prophages</i>	
0394	peptidyl-tRNA hydrolase (pth)	81	1319	ribosomal prt L35 (rpl35)	94	1690	Na ⁺ and Cl ⁻ dependent GABA transporter	53	1488	E16 prt (muE16)	53
1311	Phe-tRNA Sase α sub (pheS)	82	0778	ribosomal prt L4 (rpl4)	93	0736	Na ⁺ -dependent noradrenaline transporter	54	1503	G prt (muG)	52
1312	Phe-tRNA Sase β sub (pheT)	80	0790	ribosomal prt L5 (rpl5)	96	0504	periplasmic ribose-BP (rbsB)	57	1568	G prt (muG)	54
0729	Pro-tRNA Sase (proS)	87	0641	ribosomal prt L7/L12 (rpl7/L12)	92	1713	phosphotransferase (ptsH)	87	1493	gam prt	74
1644	pseudouridylylase I (hisT)	83	0544	ribosomal prt L9 (rpl9)	86	0828	phosphotransferase (ptsH)	80	1504	host factor-1 (HF-1) (hfq)	97
0245	queuosine biosyn prt (queA)	86	1220	ribosomal prt S1 (rps1)	89	1049	potassium channel homolog (kch)	80	1516	MuB prt (muB)	70
0200	selenium metabolism prt (selD)	80	0076	ribosomal prt S10 (rps10)	99	1109	ribose permease (xyIH)	84	1515	N prt (muN)	52
0110	Ser-tRNA Sase (serS)	86	0800	ribosomal prt S11 (rps11)	96		<i>Cations</i>		1411	terminase sub 1	82
1367	Thr-tRNA Sase (trmS)	86	0799	ribosomal prt S13 (rps13)	93	0254	bacterioferritin comigratory prt (bcp)	80	1478	transposase A (muA)	60
0202	tRNA (guanine-N1)-MTase (trmD)	93	0791	ribosomal prt S14 (rps14)	95	0251	energy transducer (tonB)	98		<i>Radiation sensitivity</i>	
0648	tRNA (U-5)-MTase (trmA)	80	1328	ribosomal prt S15 (rps15)	87	1272	ferric enterobactin transport ATP-BP (fepC)	51	0952	DNA repair prt (radC)	72
0068	tRNA δ (2)-isopentenylphosphosphate Tase (trpX)	87	1468	ribosomal prt S15 (rps15)	87	1470	ferric enterobactin transport ATP-BP (fepC)	55		<i>Transposon-related functions</i>	
1606	tRNA nucleotidyltransferase (cca)	73	0204	ribosomal prt S16 (rps16)	85		<i>Transposon-related functions</i>		1161	15 kD prt (P15)	68
0244	tRNA-guanine transglycosylase (tgt)	91	0786	ribosomal prt S17 (rps17)	94	1466	ferrichrome-iron receptor (fhuA)	49	1577	IS1016-V6	61
0637	Trp-tRNA Sase (trpS)	86	0545	ribosomal prt S18 (rps18)	95	1385	ferritin like prt (rsgA)	74	1329	IS1016-V6	75
1610	Tyr-tRNA Sase (tyrS)	73	0781	ribosomal prt S19 (rps19)	98	1384	ferritin like prt (rsgA)	79	1018	IS1016-V6	94
1391	Val-tRNA Sase (vals)	83	0913	ribosomal prt S2 (rps2)	89	0271	iron(III) dicitrate permease (fecD)	61		<i>Other</i>	
			0531	ribosomal prt S21 (rps21)	87	1361	iron(III) dicitrate transport ATP-BP (fecE)	56	1161	15 kD prt (P15)	68
			0783	ribosomal prt S3 (rps3)	93	1035	magnesium and cobalt transport prt (cofA)	85	0085	2-hydroxyacid dehydrogenase (dhH)	73
			0801	ribosomal prt S4 (rps4)	95	0097	major ferric iron-BP precursor (fbp)	82	0460	β -lactamase regulatory prt (mazG)	73
			0795	ribosomal prt S5 (rps5)	96	1049	mercury transport prt (merT)	54	0680	chloramphenicol-sensitive prt (radD)	53
			0547	ribosomal prt S8 (rps6)	87	1050	mercury scavenger prt (merP)	46	1670	conjugative transfer co-repressor (finC)	52
			1531	ribosomal prt S6 modification prt (rimK)	69	0292	mercury scavenger prt (merP)	67	0307	δ -1-pyrroline-5-carboxylate RDase (procC)	60
			0580	ribosomal prt S7 (rps7)	94	1525	molybdate-BP (modB)	43	1549	heterocyst maturation prt (devA)	66
			0792	ribosomal prt S8 (rps8)	91	0427	Na ⁺ ,H ⁺ antiporter (nhaB)	87	1577	embryonic abundant prt, group 3	89
			1442	ribosomal prt S9 (rps9)	98	1107	Na ⁺ ,H ⁺ antiporter (nhaC)	62	0916	export factor homolog (skp)	76
			0010	ribosomal prt-Ala acetyltransferase (rimI)	73	0225	Na ⁺ ,H ⁺ antiporter 1 (nhaA)	75	0587	extragenic suppressor (suhB)	80
			0581	streptomycin resistance prt (strA)	100	0098	periplasmic-BP-dependent iron transport (sfuB)	59	1013	glyoxylate-induced prt (glpX)	63
						1474	periplasmic-BP-dependent iron transport (sfuC)	58	0497	heat shock prt (hsiU)	89
						0911	potassium efflux system (kefC)	66	1119	ilv-related prt	77
						0290	potassium, copper-transporting ATPase A (copA)	64	0285	isochorismate Sase (atnC)	49
						1352	sodium, Pro symporter (putP)	79	1618	membrane assoc ATPase (cbiO)	53
						0625	TRK system potassium uptake prt (trkA)	83	0461	membrane prt (lapB)	56
							<i>Nucleosides, purines and pyrimidines</i>		1119	membrane prt (lapB)	56
						1087	ribonucleotide transport ATP-BP (mkl)	61	0630	mucoid status locus prt (mucB)	52
						1227	uracil permease (uraA)	62	0588	N-carbamyl-L-amino acid amidohydrolase	59
							<i>Other</i>		1295	nitrogen fixation prt (nifS)	56
						0621	ATP-BP (abc)	73	1343	nitrogen fixation prt (nifS)	59
						0060	ATP-dependent translocator (msbA)	100	0377	nitrogen fixation prt (nifU)	74
						1619	cystic fibrosis transmembrane conductance regulator	61	0378	nitrogen fixation prt (nifV)	74
						0853	heme-binding lpp (dppA)	99	1296	nitrogen fixation prt (nifE)	48
						0264	heme-hemopexin-BP (hxaA)	89	0179	nitrogenase C (nifC)	53
						1471	hemin permease (hemU)	99	1425	nitrogenase C (nifC)	60
						0262	hemin precursor precursor (hemR)	64	1296	partitioning system prt (parB)	68
						1706	high-affinity choline transport prt (betT)	62	0556	putative glucose-6-P DHase isozyme (devB)	94
						0661	lactoferrin-BP (lbpA)	48	0981	small prt (smpB)	91
						0608	Na ⁺ , sulfate cotransporter	86	1592	spolIIE prt (spolIIE)	75
						00975	pantothenate permease (panF)	76	0095	spore germination and vegetative growth prt (gerC2)	56
						00973	transferrin-BP (tfbA)	48	0896	suppressor prt (msgA)	56
						0712	transferrin-BP 1 (tbp1)	49	1078	surfactin (sfpo)	78
						1565	transferrin-BP 1 (tbp1)	59	0357	thiamine-repressed prt (nmt1)	55
						0394	transferrin-BP 1 (tbp1)	59	0751	toxR regulon (tagD)	64
						1217	transferrin-BP 1 (tbp1)	52	1401	trnN	62
						0635	transferrin-BP 2 (tbp2)	55	0664	transport ATP-BP (cydC)	52
						0663	transport ATP-BP (cydD)	54	1156	transport ATP-BP (cydC)	70
						1157	transport ATP-BP (cydD)	73	1556	vanamycin-resistance prt (vanH)	57
							<i>Other categories</i>				
							<i>Adaptations and atypical conditions</i>				
						1526	autotrophic growth prt (aut)	61			
						0071	heat shock prt B253 (grpE)	66			
						0720	heat shock prt (htpX)	82			
						1527	heat shock prt B (hspB)	71			
						0945	htrA-like prt (htrH)	73			
						0901	invasion prt (invA)	61			
						1544	NAD(P)H:menadiene oxidoreductase	55			
						0458	survival prt (surA)	58			
						0815	universal stress prt (uspA)	87			
						1251	virulence assoc prt A (vapA)	58			
						0322	virulence assoc prt C (vapC)	57			
						0947	virulence assoc prt C (vapC)	61			
						0450	virulence assoc prt D (vapD)	67			
						1307	virulence plasmid prt (mlgA)	56			
						0321	virulence plasmid prt (vagC)	58			
							<i>Colicin-related functions</i>				
						0352	colicin tolerance prt (tolB)	78			
						1205	colicin V production prt (cvpA)	79			
						0384	inner membrane prt (tolP)	79			
						0385	inner membrane prt (tolQ)	83			
						1685	outer membrane integrity prt (toaA)	48			
						0383	outer membrane integrity prt (toaA)	57			
							<i>Drug and analog sensitivity</i>				
						0895	acriflavine resistance prt (acrB)	55			
						0300	ampD signalling prt (ampD)	75			
						1242	bicyclomycin resistance prt (bcr)	69			
						1623	mercury resistance regulatory prt (merF2)	58			
						0686	glycerol-3-phosphatase transporter (glpT)	79			
						0502	high affinity ribose transport prt (rbsA)	85			
						0503	high affinity ribose transport prt (rbsC)	86			
						0501	high affinity ribose transport prt (rbsD)	78			

SCIENCE

The Genome of *Haemophilus influenzae* Rd

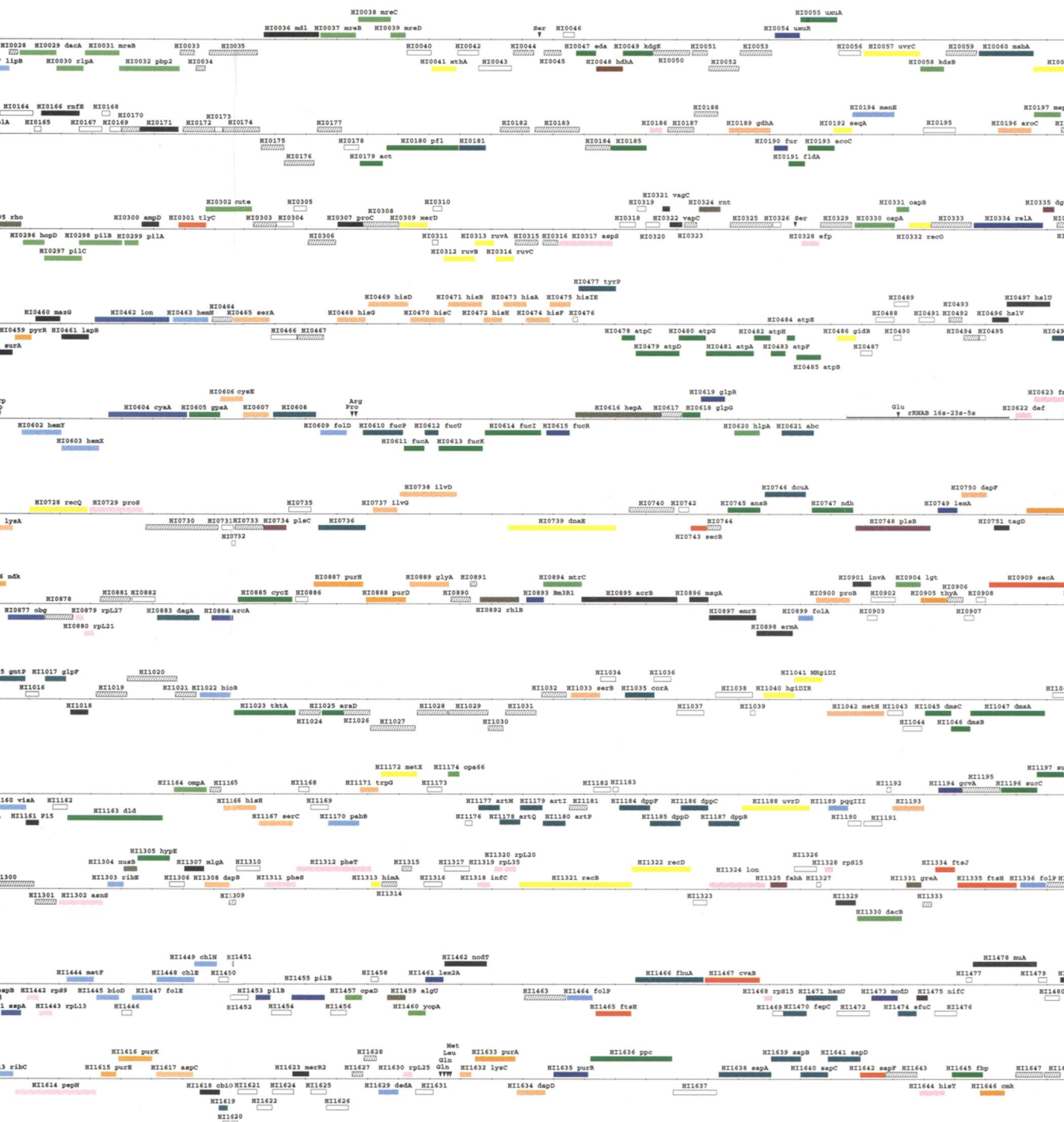
Figure 2. Gene map of the *H. influenzae* Rd genome. Predicted coding regions are shown on each strand. The rRNA and tRNA genes are shown as lines and triangles, respectively. Genes are color-coded by role category as described in the Figure key. Gene identification numbers correspond to those in Table 3. Where possible, three-letter designations are also provided. In the region containing ribosomal proteins

HI0782-HI0796 some identification numbers have been omitted because of space limitations. Predicted coding regions with similarity to database sequences designated as hypothetical coding regions are represented as white, cross-hatched rectangles. Predicted coding regions that have no database match are represented as white, unfilled rectangles.

Table 3. Identification of *H. influenzae* genes. Gene identification numbers are listed with the prefix HI in Fig. 3. Each identified gene is listed in its role category [adapted from Riley (36)]. The percentage of similarity (Sim) of the best match to the NRBP (as described in the text) is also shown. The amino acid substitution matrix used in the BLAZE analysis is BLOSUM60. An expanded version of this table with additional match information, including species, is available via World Wide Web (URL: <http://www.tigr.org/>). Abbreviations used: Ac, acetyl; ATase, aminotransferase; BP, binding protein; biosyn, biosynthesis; CoA, coenzyme A; DCase, decarboxylase; DHase, dehydrogenase; DMSO, dimethyl sulfoxide; f-Met, formylmethionine; G3PD, glyceraldehyde-3-phosphate dehydrogenase; GABA, γ -aminobutyric acid; GlcNAc, *N*-acetylglucosamine; LOS, Lipooligosaccharide; lpp, lipoprotein; MTase, methyltransferase; MurNAc, *N*-acetylmuramyl; P, phosphate; prt, protein; PRTase, phosphoribosyltransferase; RDase, reductase; SAM, *S*-adenosylmethionine; Sase, synthase-synthetase; sub, subunit; Tase, transferase. The following hypothetical proteins were matched from the other species as indicated (percent similarity in parentheses after gene identification number): *Alcaligenes eutrophus*: 1053(52); *Anabaena variabilis*: 1349(54); *Bacillus subtilis*: 0115(53), 0259(54), 0355(61), 0404(47), 0415(69), 0416(63), 0417(66), 0454(64), 0456(56), 0522(54), 0687(49), 0775(54), 0959(50), 1083(53), 1203(63), 1627(59), 1647(81), 1648(65), 1654(64); Bacteriophage P22: 1412(54); *Buchnera aphidicola*: 1199(65); *Campylobacter jejuni*: 0560(71); *Chromatium vinosum*: 0105(75); *Clostridium acetobutylicum*: 0773(72); *Clostridium kluveri*: 0976(48); *Clostridium perfringens*: 0143(58); *Coxiella burnetii*: 1590(74), 1591(50); *Erwinia carotovora*: 1436(72); *Escherichia coli*: 0003(52), 0012(67), 0017(91), 0028(68), 0033(90), 0034(84), 0035(79), 0044(80), 0045(67), 0050(70), 0051(50), 0052(56), 0053(56), 0059(72), 0065(75), 0072(65), 0081(71), 0091(72), 0092(49), 0093(59), 0103(71), 0107(54), 0108(65), 0125(88), 0126(87), 0135(68), 0145(69), 0146(58), 0147(61), 0148(62), 0162(47), 0172(67), 0174(84), 0175(70), 0176(87), 0182(60), 0183(66), 0184(73), 0187(58), 0188(81), 0198(75), 0203(86), 0227(51), 0230(71), 0232(69), 0235(80), 0241(82), 0242(50), 0258(95), 0257(76), 0265(77), 0266(83), 0270(80), 0271(73), 0276(70), 0281(76), 0282(59), 0293(61), 0303(81), 0306(70), 0308(58), 0315(87), 0316(68), 0329(79), 0336(91), 0338(68), 0340(72), 0341(84), 0342(60), 0343(67), 0344(85), 0345(82), 0346(77), 0347(67), 0364(55), 0365(86), 0367(48), 0371(84), 0374(64), 0375(62), 0376(75), 0379(57), 0380(58), 0386(76);

0393(93), 0396(54), 0398(72), 0400(65), 0409(69), 0412(85), 0418(68), 0423(67), 0424(66), 0431(76), 0432(68), 0442(93), 0452(73), 0464(78), 0467(80), 0493(64), 0494(69), 0500(63), 0508(82), 0509(69), 0510(74), 0519(71), 0520(59), 0521(58), 0562(83), 0565(63), 0568(71), 0570(80), 0572(70), 0574(63), 0575(80), 0576(65), 0597(57), 0617(54), 0624(72), 0626(81), 0634(78), 0638(68), 0647(64), 0656(74), 0658(56), 0668(76), 0670(83), 0671(87), 0696(54), 0697(64), 0700(77), 0702(71), 0719(86), 0721(78), 0723(73), 0724(64), 0730(65), 0733(55), 0744(70), 0755(61), 0756(60), 0766(87), 0767(72), 0810(74), 0817(68), 0826(70), 0827(86), 0831(77), 0837(74), 0839(69), 0840(72), 0841(66), 0849(75), 0851(71), 0852(66), 0855(75), 0858(68), 0860(86), 0862(81), 0864(92), 0878(71), 0881(81), 0890(69), 0891(79), 0906(71), 0918(81), 0929(58), 0933(71), 0934(52), 0935(63), 0936(64), 0943(83), 0948(67), 0955(72), 0956(73), 0963(67), 0965(81), 0979(79), 0984(79), 0986(81), 0988(85), 1000(80), 1001(75), 1005(61), 1007(86), 1010(53), 1019(65), 1020(65), 1021(71), 1024(67), 1026(85), 1027(72), 1028(77), 1029(83), 1030(62), 1031(87), 1032(79), 1064(57), 1072(57), 1073(62), 1082(67), 1084(61), 1085(76), 1086(89), 1089(70), 1090(82), 1091(76), 1092(73), 1093(72), 1094(81), 1095(79), 1096(64), 1104(53), 1118(84), 1125(87), 1129(77), 1130(80), 1146(80), 1147(68), 1148(88), 1149(73), 1150(59), 1151(81), 1153(84), 1155(79), 1165(87), 1181(68), 1195(76), 1198(85), 1216(73), 1234(80), 1240(77), 1243(74), 1252(93), 1262(61), 1280(71), 1282(74), 1288(84), 1289(74), 1297(67), 1298(69), 1300(58), 1301(82), 1309(67), 1314(70), 1315(66), 1333(79), 1337(84), 1342(57), 1364(56), 1368(53), 1369(44), 1437(72), 1463(84), 1542(61), 1545(80), 1558(62), 1598(58), 1608(76), 1612(72), 1628(61), 1643(70), 1652(68), 1653(88), 1655(56), 1656(69), 1657(65), 1664(50), 1677(72), 1679(69), 1703(74), 1704(73), 1714(78), 1715(86), 1721(71), 1723(92); *Klebsiella pneumoniae*: 0021(63); *Lactobacillus johnsonii*: 0112(54), 1720(55); *Lactococcus lactis*: 0555(69); *Mycobacterium leprae*: 0004(62), 0019(62), 0136(58), 0260(56), 0694(54), 0740(56), 0920(57), 1663(55); *Mycoplasma hyopneumoniae*: 1281(71); *Pasteurella haemolytica*: 0219(92); *Pseudomonas aeruginosa*: 0090(68), 0177(56); *Rhodobacter capsulatus*: 0170(62), 0672(59), 1439(65), 1683(75), 1684(60), 1688(58); *Salmonella typhimurium*: 0405(51), 0964(67), 1434(76), 1607(51); *Shigella flexneri*: 0277(52); *Streptococcus parasanguis*: 0359(65); *Synechococcus* sp.: 0961(70); *Vibrio parahaemolyticus*: 0323(87), 0325(75); *Vibrio* sp.: 0333(70); *Yersinia enterocolitica*: 0753(69).

Hit#	Identification	%Sim	Hit#	Identification	%Sim	Hit#	Identification	%Sim	Hit#	Identification	%Sim
Amino acid biosynthesis											
<i>Aromatic amino acid family</i>											
0970	3-dehydroquinase (aroQ)	83	0457	aminodeoxychorismate lyase (pabC)	67	1139	UDP-MurNAc-Ala ligase (murC)	82	0445	protein-export membrane prt (secG)	81
0208	amidotransferase (aroB)	77	1629	dedA	55	1136	UDP-MurNAc-Ala-D-Glu ligase (murD)	74	0743	protein-export prt (secB)	81
0472	amidotransferase (hisH)	70	0699	dehydrofolate RDase, type I (foIA)	68	1134	UDP-MurNAc-pentapeptide Sase (murF)	68	0809	preprotein translocase sub (secA)	82
1387	anthranilate Sase component I (trpE)	73	1336	dihydropterolate Sase (foiP)	71	1133	UDP-MurNAc-tripeptide Sase (murE)	73	0151	signal peptidase I (lepB)	65
1388	anthranilate Sase component II (trpD)	74	1464	dihydropterolate Sase (foiP)	68	0268	UDP-NAC-enolpyruvylglucosamine RDase (murB)	76	0106	signal recognition particle prt 54 (fth)	91
1389	anthranilate isomerase (trpC)	73	1447	GTP cyclohydrolase I (foiE)	79				0713	trig factor (fig)	80
1171	anthranilate Sase Gln amidotransferase (trpG)	59	1170	p-aminobenzoate Sase (pabB)	54	<i>Surface polysaccharides, lipopolysaccharides and antigens</i>					
0468	ATP PRTase (hisG)	82	<i>Heme and porphyrin</i>			1557	2-dehydro-3-deoxyphosphoconate aldolase (kdsA)	92	<i>Transformation</i>		
1250	chorismate mutase-prephenate dehydratase (pheA)	77	1160	ferrochelatase (visA)	69	0652	3-deoxy-D-manno-octulosonic-acid Tase (kdtA)	70	1008	competence locus E (comE1)	70
0196	chorismate Sase (aroC)	88	0113	heme utilization prt (hxcU)	46	1105	ADP-heptose-1ps heptosyltransferase II (raF)	79	0601	ifoX	100
1547	DAH P Sase (aroG)	84	0263	heme-hemopexin utilization (hxcB)	99	1114	ADP-L-glycero-D-mannoheptose-6-epimerase (raD)	88	0439	transformation prt (comA)	100
0607	dehydroquinase shikimate DHase	48	0463	oxygen-independent coproporphyrinogen III oxidase (hemN)	52	0058	CTP:OMP-3-deoxy-D-manno-octulosonate-cytidyl-yl-transferase (kdsB)	82	0438	transformation prt (comB)	100
1589	enolpyruvylshikimatephosphateSyn (aroA)	98	0602	protoporphyrinogen oxidase homolog	64	0668	glycosyl Tase (igtD)	55	0437	transformation prt (comC)	100
1166	Gln amidotransferase (hisH)	61	1201	protoporphyrinogen oxidase (hemG)	57	1578	glycosyl Tase (igtD)	64	0436	transformation prt (comD)	100
0469	histidinol dehydrogenase (hisD)	78	1559	protoporphyrinogen oxidase (hemG)	73	1539	lic-1 operon prt (licA)	99	0435	transformation prt (comE)	100
0474	hisF cyclase (hisF)	91	0603	uroporphyrinogen III methylase (hemX)	60	1538	lic-1 operon prt (licB)	99	0434	transformation prt (comF)	100
0470	histidinol-P ATase (hisC)	77	<i>Lipoate</i>			1678	kpsF prt (kpsF)	84	Central intermediary metabolism		
0471	imidazoleglycerol-P dehydratase (hisB)	81	0026	lipoate biosyn prt A (lipA)	84	1537	lic-1 operon prt (licA)	100	<i>Amino sugars</i>		
0475	phosphoribosyl-AMP cyclohydrolase (hisI)	77	0027	lipoate biosyn prt B (lipB)	84	1538	lic-1 operon prt (licB)	99	0140	GlcNAc-6-P deacetylase (nagA)	72
0473	phosphoribosylformimino-5-aminimidazole carboximidate ribotide isomerase (hisA)	77	<i>Menaquione and ubiquinone</i>			1539	lic-1 operon prt (licC)	99	0429	Gln amidotransferase (glmS)	84
0655	shikimate 5-DHase (aroE)	70	0283	2-succinyl-6-hydroxy-2,4-cyclohexadiene-1-carboxylate Sase (menD)	64	1540	lic-1 operon prt (licD)	94	0141	glucosamine-6-P deaminase (nagB)	88
0207	shikimate acid kinase I (aroK)	88	0969	4-(2'-carboxyphenyl)-4-oxybutyric acid Sase (menC)	74	1060	lipid A disaccharide Sase (lpxB)	77	<i>Degradation of polysaccharides</i>		
1432	Trp Sase α chain (trpA)	73	0969	4-(2'-carboxyphenyl)-4-oxybutyric acid Sase (menC)	74	0765	LOS biosyn prt	60	1356	amylomaltase (malQ)	62
1431	Trp Sase β chain (trpB)	90	1189	coenzyme PQQ synthesis prt III (pqqIII)	49	0550	LOS biosyn prt	79	<i>Other</i>		
<i>Aspartate family</i>											
0564	Asn Sase A (asnA)	77	0968	dihydroxynaphthoic acid Sase (menB)	95	1651	lipopolysaccharide core biosyn prt (kdtB)	96	0048	7- α -hydroxysteroid DHase (hdhA)	55
0296	Asp ATase (aspC)	54	1438	famesylidiphosphate Sase (spsA)	71	1700	lsg locus prt 1	100	1204	acetate kinase (ackA)	84
1617	Asp ATase (aspC)	79	0194	O-succinylbenzoate-CoA Sase (menE)	67	0867	lsg locus prt 1	83	0949	GABA transaminase (gabT)	56
0646	Asp-semialdehyde DHase (asd)	65	<i>Molybdopterin</i>			1699	lsg locus prt 2	97	0111	glutathione Tase (gphH)	57
1632	aspartokinase III (lysC)	74	1676	molybdenum biosyn prt A (moaA)	78	1698	lsg locus prt 3	99	0691	glycerol kinase (gpkK)	89
1082	aspartokinase-homoserine DHase (thrA)	77	1675	molybdenum biosyn prt C (moaC)	89	1697	lsg locus prt 4	98	0584	hippuricase (hipO)	50
1042	B12-dependent homocysteine-N5-methyltetrahydrofolate transmethylase (metH)	70	1370	molybdenum-pterin-BP (mopI)	74	1696	lsg locus prt 5	98	0541	urease (ureA)	76
0122	β -cystathionase (metC)	84	1448	molybdopterin biosyn prt (chlE)	73	1695	lsg locus prt 6	99	0539	urease α sub (urea amidohydrolase)	82
0066	cystathionine γ -Sase (metB)	62	0118	molybdopterin biosyn prt (chlN)	53	1694	lsg locus prt 7	98	0581	urease β sub (urea amidohydrolase)	82
1308	dehydrodipicolinate RDase (dapB)	83	1449	molybdopterin biosyn prt (chlN)	78	1693	lsg locus prt 8	99	0537	urease accessory prt (UreF)	55
0727	diaminopimelate DCase (lysA)	79	1674	molybdopterin converting factor, sub 1 (moaD)	79	1144	UDP-3-O-acyl GlcNAc deacetylase (envA)	77	0538	urease prt (ureE)	57
0750	diaminopimelate epimerase (dapF)	86	1673	molybdopterin converting factor, sub 2 (moaE)	76	0915	UDP-3-O-(R-3-hydroxymyristoyl)-glucosamine N-acetyltransferase (firA)	79	0536	urease prt (ureG)	87
0255	dihydrodipicolinate Sase (dapA)	80	0844	molybdopterin-dinucleotide biosyn prt (mob)	62	1061	UDP-GlcNAc acetyltransferase (lpxA)	79	0535	urease prt (ureH)	88
1263	homoserine acetyltransferase (met2)	57	<i>Pantothenate</i>			0873	UDP-GlcNAc epimerase (rfiE)	79	0540	urease sub B (ureB)	77
0088	homoserine kinase (thrB)	81	0953	pantothenate metabolism flavoprotein (dtp)	77	0872	undecaprenyl-P Gal-P Tase (rfbP)	75	<i>Phosphorus compounds</i>		
0102	succinyl-diaminopimelate desuccinylase (dapE)	80	0631	pantothenate kinase (coaA)	78	<i>Surface structures</i>					
1634	tetrahydrodipicolinate N-succinyltransferase (dapD)	99	<i>Pyridoxine</i>			0119	adhesin B precursor (fimA)	48	0695	exopolyphosphatase (ppx)	77
1702	tetrahydropteroyltryglutamate MTase (metE)	68	0863	pyridoxamine phosphate oxidase (pdxH)	65	0362	adhesin B precursor (fimA)	78	0124	inorganic PPase (ppa)	50
0087	Thr Sase (thrC)	81	<i>Riboflavin</i>			0330	cell envelope prt (oapA)	100	0645	lysophospholipase L2 (pldB)	53
<i>Branched chain family</i>											
0969	3-isopropylmalate dehydratase (leuD)	85	0764	3,4-dihydroxy-2-butanone 4-P Sase (ribB)	83	0331	opacity assoc prt (oapB)	99	<i>Polysaccharides - (cytoplasmic)</i>		
0967	3-isopropylmalate DHase (leuB)	80	0212	GTP cyclohydrolase II (ribA)	81	1174	opacity prt (opa66)	51	1357	1,4- α -glucan branching enzyme (glgB)	80
0737	acetoaldehyde Sase II (livG)	79	0944	riboflavin biosyn prt (ribG)	76	0414	opacity prt (opa66)	59	1361	α -glucan phosphorylase (glgP)	79
1585	acetoaldehyde Sase III large chain (livI)	84	1613	riboflavin Sase α chain (ribC)	82	1457	opacity prt (opaD)	56	1359	ADP-glucose Sase (glgC)	74
1584	acetoaldehyde Sase III small chain (livH)	85	1303	riboflavin Sase β chain (ribE)	90	1460	outer membrane adhesin (yopA)	62	1358	glucogen operon prt (glgX)	68
1193	branched-chain amino acid transaminase	49	<i>Thioredoxin, glutaredoxin, and glutathione</i>			0299	pilin biogenesis prt (pilA)	52	1356	glucogen operon prt (glgX)	68
0738	dihydroxyacid dehydratase (livD)	90	0161	glutathione RDase (gor)	85	0628	pilin biogenesis prt (pilB)	65	1360	glucogen Sase (glgA)	71
0963	α -isopropylmalate Sase (leuA)	100	1115	thioredoxin (trxA)	59	0298	pilin biogenesis prt (pilB)	62	<i>Sulfur metabolism</i>		
0682	ketol acid reductoisomerase (livC)	90	1159	thioredoxin (trxA)	62	0297	pilin biogenesis prt (pilC)	57	0805	arsulfolatase regulatory prt (asIB)	67
Cell envelope											
<i>Membranes, lipoproteins, and porins</i>											
<i>Glutamate family</i>											
0811	argininosuccinate lyase (argH)	84	0084	thioredoxin m (trxM)	79	Cellular processes					
1727	argininosuccinate Sase (argG)	87	<i>Cell division</i>			0119	adhesin B precursor (fimA)	48	0699	nucliotide-BP (potG)	67
0900	γ -glutamyl kinase (proB)	80	0769	cell division ATP-BP (ftsE)	78	0362	adhesin B precursor (fimA)	78	0591	omithine DCase (speF)	80
1239	γ -glutamyl-P RDase (proA)	79	1208	cell division inhibitor (sulA)	56	0330	cell envelope prt (oapA)	100	<i>Polysaccharides - (cytoplasmic)</i>		
0665	Gln Sase (glnA)	86	1142	cell division prt (ftsA)	74	0331	opacity assoc prt (oapB)	99	1357	1,4- α -glucan branching enzyme (glgB)	80
0189	Glu DHase (gdhA)	84	1335	cell division prt (ftsH)	74	1174	opacity prt (opa66)	51	1361	α -glucan phosphorylase (glgP)	79
0596	omithine carbamoyltransferase (arcB)	91	1465	cell division prt (ftsH)	74	0414	opacity prt (opa66)	59	1359	ADP-glucose Sase (glgC)	74
1719	uridylyl Tase (glnD)	68	1334	cell division prt (ftsJ)	74	1457	opacity prt (opaD)	56	1358	glucogen operon prt (glgX)	68
<i>Pyruvate family</i>											
1575	Ala racemase, biosynthetic (alr)	75	1460	outer membrane adhesin (yopA)	62	0414	opacity prt (opa66)	59	0535	urease prt (ureH)	88
<i>Serine family</i>											
1102	Cys Sase (cysZ)	76	0299	pilin biogenesis prt (pilA)	52	1174	opacity prt (opa66)	51	0540	urease sub B (ureB)	77
1103	Cys Sase (cysK)	84	0628	pilin biogenesis prt (pilB)	65	1460	outer membrane adhesin (yopA)	62	<i>Phosphorus compounds</i>		
0465	phosphoglycerate DHase (serA)	84	0298	pilin biogenesis prt (pilB)	62	0915	UDP-3-O-(R-3-hydroxymyristoyl)-glucosamine N-acetyltransferase (firA)	79	0695	exopolyphosphatase (ppx)	77
1167	phosphoserine ATase (serC)	72	1021	leukotoxin secretion ATP-BP (lktB)	65	0873	UDP-GlcNAc epimerase (rfiE)	79	0124	inorganic PPase (ppa)	50
1033	phosphoserine phosphatase (serB)	70	<i>Murein sacculus and peptidoglycan</i>			0872	undecaprenyl-P Gal-P Tase (rfbP)	75	0645	lysophospholipase L2 (pldB)	53
0606	Ser acetyltransferase (cysE)	88	1140	D-Ala-D-Ala ligase (ddlB)	76	<i>Surface structures</i>					
0689	Ser hydroxymethyltransferase (glyA)	94	1330	D-alanyl-D-Ala carboxypeptidase (dacB)	68	0119	adhesin B precursor (fimA)	48	0699	nucliotide-BP (potG)	67
Biosynthesis of cofactors, prosthetic groups, and carriers											
<i>Biotin</i>											
1554	7,8-diamino-pelargonic acid ATase (bioA)	74	1494	MurNAc-L-Ala amidase	62	0330	cell envelope prt (oapA)	100	0591	omithine DCase (speF)	80
1553	7-keto-8-aminopelargonic acid Sase (bioF)	56	0066	N-acetylmuramoyl-L-Ala amidase (amiB)	77	0331	opacity assoc prt (oapB)	99	1357	1,4- α -glucan branching enzyme (glgB)	80
1551	biotin synthesis prt (bioC)	47	0440	penicillin-BP (ponA)	100	1174	opacity prt (opa66)	59	1361	α -glucan phosphorylase (glgP)	79
0643	biotin sulfoxide RDase (bisC)	72	1725	penicillin-BP 1B (ponB)	67	1457	opacity prt (opaD)	56	1359	ADP-glucose Sase (glgC)	74
1022	biotin Sase (bioB)	78	0032	penicillin-BP 2 (ppb2)	74	1460	outer membrane adhesin (yopA)	62	1358	glucogen operon prt (glgX)	68
1550	dethiobiotin Sase (bioD)	60	1668	penicillin-BP 3 (prc)	70	0299	pilin biogenesis prt (pilA)	52	1356	glucogen operon prt (glgX)	68
1445	dethiobiotin Sase (bioD)	62	0029	penicillin-BP 5 (dacA)	68	0197	penicillin-insensitive murein endopeptidase (mepA)	67	0535	urease prt (ureH)	88
<i>Folic acid</i>											
1444	5,10-methylenetetrahydrofolate RDase (metF)	83	0381	peptidoglycan-assoc outer membrane lpp	100	1135	phospho-N-acetylmuramoyl-pentapeptide-Tase E (mraY)	89	0540	urease sub B (ureB)	77
0609	5,10-methylenetetrahydrofolate DHase (folD)	82	0031	rod shape-determining prt (mreB)	81	0031	rod shape-determining prt (mreB)	81	0695	exopolyphosphatase (ppx)	77
0064	7,8-dihydro-6-hydroxymethylpterin-pyrophosphokinase (folK)	78	0037	rod shape-determining prt (mreB)	90	0038	rod shape-determining prt (mreC)	74	0124	inorganic PPase (ppa)	50
			0039	rod shape-determining prt (mreC)	74	0039	rod shape-determining prt (mreD)	72	0645	lysophospholipase L2 (pldB)	53
			0829	soluble lytic murein transglycosylase (slt)	59	0039	rod shape-determining prt (mreD)	72	0695	exopolyphosphatase (ppx)	77
			1081	UDP-GlcNAc enolpyruvyl Tase (murZ)	85	0239	protein-export membrane prt (secD)	73	0124	inorganic PPase (ppa)	50
						0239	protein-export membrane prt (secF)	73	0645	lysophospholipase L2 (pldB)	53



- Amino acid biosynthesis
- Biosynthesis of cofactors, prosthetic groups, carriers
- Cell envelope
- Cellular processes
- Central intermediary metabolism
- Energy metabolism
- Fatty acid/Phospholipid metabolism
- Purines, pyrimidines, nucleosides and nucleotides
- Regulatory functions
- Replication

3) The two λ libraries constructed from *H. influenzae* genomic DNA were probed with oligonucleotides designed from the ends of contig groups (27). The positive plaques were then used to prepare templates, and the sequence was determined from each end of the λ clone insert. These sequence fragments were searched with GRASTA against a database of all contigs. Two contigs that matched the sequence from the opposite ends of the same λ clone were ordered. The λ clone then provided the template for closure of the sequence gap between the adjacent contigs.

4) To confirm the order of contigs found by the other approaches and establish the order of the remaining contigs, we performed amplifications by polymerase chain reaction (PCR), both standard and long range (XL) (28). Although a PCR reaction was done for essentially every combination of physical gap ends, techniques such as DNA fingerprinting, database matching, and the probing of large insert clones were particularly valuable in ordering contigs adjacent to each other and reducing the number of combinatorial PCRs necessary to achieve complete gap closure. Use of these strategies to an even greater extent in future genome projects will increase the overall efficiency of complete genome closure. In the program ASM_ALIGN Southern analysis data, identification of peptide links, forward and reverse sequence data from λ clones, and PCR data are used to establish the relative order of the contigs separated by physical gaps. The number of physical gaps ordered and closed by each of these techniques is summarized in Table 2.

Lambda clones were a central feature for completion of the genome sequence and assembly. It was probable that some fragments of the *H. influenzae* genome would be nonclonable in a high copy plasmid because they would produce deleterious proteins in the *E. coli* host cells. Lytic λ clones would provide DNA for these segments because such genes would not inhibit plaque production. Furthermore, sequence information from the ends of 15- to 20-kb clones is particularly suitable for gap closure and providing general confirmation of genome assembly. Because of their size, they would be likely to span any physical gap. Approximately 100 random plaques were picked from the amplified λ library, templates were prepared, and sequence information was obtained from each end. These sequences were searched (GRASTA) against the contigs and linked in the database to their appropriate contig, thus providing a scaffolding of λ clones that contributed additional support to the accuracy of the genome assembly (Fig. 1). In addition to confirmation of the contig structure, the λ clones provided closure for 23 physical gaps.

Approximately 78 percent of the genome was covered by λ clones.

The λ clones were particularly useful for solving repeat structures. All repeat structures identified in the genome were small enough to be spanned by a single clone from the random insert library, except for the six ribosomal RNA (rRNA) operons and one repeat (two copies) that was 5340 bp in length. The ability to distinguish and assemble the six rRNA operons of *H. influenzae* (each containing in order 16S, 23S, and 5S subunit genes) was a test of our overall strategy to sequence and assemble a complex genome that might contain a significant number of repeat regions. The high degree of sequence similarity and the length of the six operons caused the assembly process to cluster all the underlying sequences into a few indistinguishable contigs. To de-

termine the correct placement of the operons in the sequence, unique sequences were identified at the 5S ends. Oligonucleotide primers were designed from these six flanking regions and used to probe the two λ libraries. For five of the six rRNA operons at least one positive plaque was identified that completely spanned the rRNA operon and contained uniquely identifying flanking sequence at the 16S and 5S ends. These plaques provided the templates for obtaining the sequence for these rRNA operons. For *rrnA* a plaque was identified that contained the particular 5S end and terminated in the 16S end. The 16S end of *rrnA* was obtained by PCR from *H. influenzae* Rd genomic DNA.

An additional confirmation of the global structure of the assembled circular genome was obtained by comparing a computer-

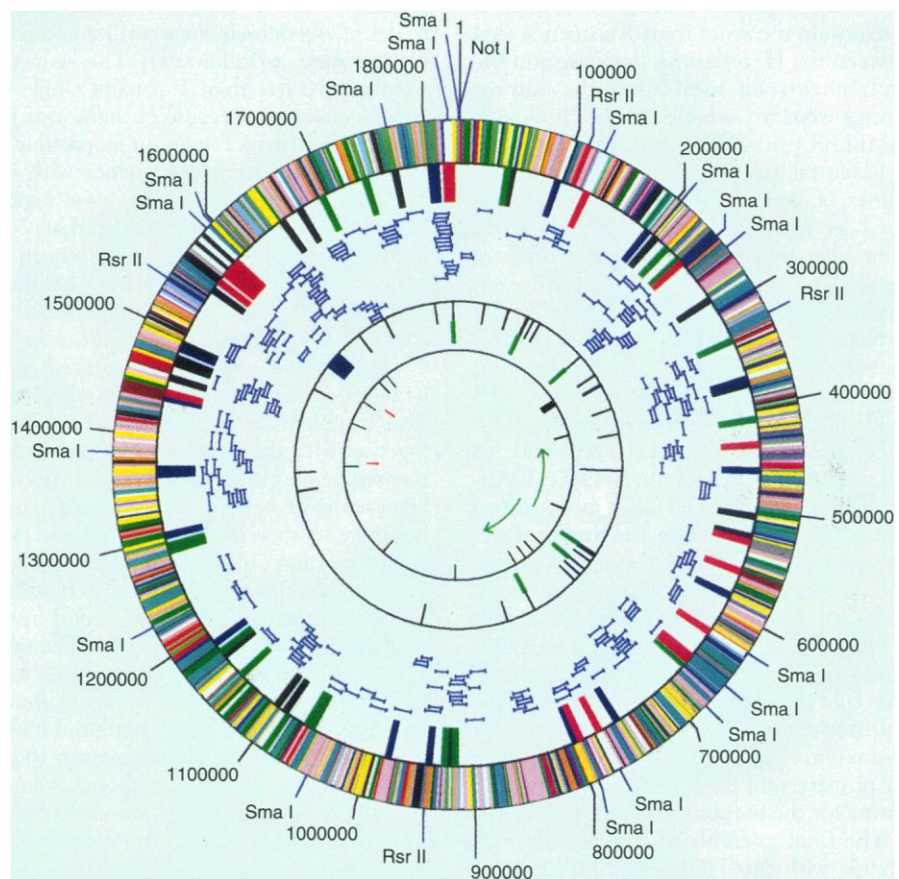


Fig. 1. A circular representation of the *H. influenzae* Rd chromosome illustrating the location of each predicted coding region containing a database match as well as selected global features of the genome. Outer perimeter: The location of the unique Not I restriction site (designated as nucleotide 1), the Rsr II sites, and the Sma I sites. Outer concentric circle: Coding regions for which a gene identification was made. Each coding region location is classified as to role according to the color code in Fig. 2. Second concentric circle: Regions of high G+C content (>42 percent, red; >40 percent, blue) and high A+T content (>66 percent, black; >64 percent, green). Third concentric circle: Coverage by λ clones (blue). More than 300 λ clones were sequenced from each end to confirm the overall structure of the genome and identify the six ribosomal operons. Fourth concentric circle: The locations of the six ribosomal operons (green), the tRNAs (black) and the cryptic mu-like prophage (blue). Fifth concentric circle: Simple tandem repeats. The locations of the following repeats are shown: CTGGCT, GTCT, ATT, AATGGC, TTGA, TTGG, TTAT, TTATC, TGAC, TCGTC, AACC, TTGC, CAAT, CCAA. The putative origin of replication is illustrated by the outward pointing arrows (green) originating near base 603,000. Two potential termination sequences are shown near the opposite midpoint of the circle (red).

generated restriction map based on the assembled sequence for the endonucleases Apa I, Sma I, and Rsr II with the predicted physical map of Lee *et al.* (29). The restriction fragments from the sequence-derived map matched those from the physical map in size and relative order (Fig. 1).

At the same time that the final gap filling process occurred, each contig was edited visually by reassembling overlapping 10-kb sections of contigs by means of the AB AUTOASSEMBLER and the Fast Data Finder hardware. AUTOASSEMBLER provides a graphical interface to electropherogram data for editing. The electropherogram data was used to assign the most likely base at each position. Where a discrepancy could not be resolved or a clear assignment made, the automatic base calls were initially left unchanged. Individual sequence changes were written to the electropherogram files and a program was designed (CRASH) to maintain the synchrony of sequence data between the *H. influenzae* database and the electropherogram files. After the editing, contigs were reassembled with TIGR ASSEMBLER prior to annotation.

Potential frameshifts identified in the course of annotating the genome were saved as reports in the database. These frameshifts were used to indicate areas of the sequence that might require further editing or sequencing. Frameshifts were not corrected for cases in which clear electropherogram data disagreed with a frameshift. Frameshift editing was done with TIGR EDITOR. This program was developed as a collaborative effort between TIGR and AB and is a modification of the AB AUTOASSEMBLER. TIGR EDITOR can download contigs from the database and thus provides a graphical interface to the electropherogram for the purpose of editing data associated with the aligned sequence file output of TIGR ASSEMBLER. The program maintains synchrony between the electropherogram files on the Macintosh system and the sequence data in the *H. influenzae* database on the Unix system. TIGR EDITOR is now our primary tool for sequence viewing and editing for the purpose of genome assembly.

The final assembly of the *H. influenzae* genome with the TIGR ASSEMBLER was precluded by the rRNA and other repeat regions, and was accomplished by means of COMB_ASM (a program written at TIGR) that splices together contigs on the basis of short sequence overlaps.

Throughout the project, we paid particular attention to the accuracy of the sequence generated and included various quality control measures. In particular, we constructed random small and large insert libraries (as described above), used strict criteria for excluding any single sequence in which more than 3 percent of the nucleo-

tides could not be identified with certainty, determined that there was no vector contamination in each sequence, and rejected chimeric sequences from the assembly process. The most important measure of the sequence accuracy is the correct assembly of the 1.8-Mb genome. Any deviation from inclusion of only high-quality sequences would have resulted in an inability to assemble the final genome. In addition, the use of the large insert λ clones confirmed the accuracy of the final assembly. Our finding that the restriction map of the *H. influenzae* Rd genome based on our sequence data is in complete agreement with that previously published (29) further confirms the accuracy of the assembly.

As a consequence of our shotgun approach, we reached an average of more than sixfold redundancy across the genome, although there are some regions in which the coverage is lower. The criteria that we used to define overall sequence quality and completion were as follows: (i) The sequence should have less than 1 percent single sequence coverage. Because *H. influenzae* is a genome rich in AT pairs, it is possible to obtain a highly accurate sequence with single-pass coverage. However, any regions with single sequence coverage that contained ambiguities were again sequenced with an alternative sequencing chemistry. (ii) Areas with more than single sequence coverage that contained ambiguities or G-C compressions were also sequenced again with an alternative sequencing chemistry. The combination of sequence redundancy together with the application of an alternative sequencing chemistry in areas with ambiguities is, we believe at least as accurate, if not more so, than double-stranded coverage. By these criteria we have reduced the number of nucleotide ambiguities [International Union of Biochemistry (IUB) codes] in the sequence to less than 1 in 19,000. The same approaches used to resolve ambiguities were also applied to areas where apparent frameshifts were indicated. Sixty potential frameshifts were identified by comparison to entries in peptide databases. Although some of these potential frameshifts are undoubtedly real, others may reflect the hundreds of frameshifts present in GenBank sequences from public databases (30). They may also represent biologically significant phenomena such as insertions or deletions in insertion elements, or in tandem repeats often associated with virulence genes (31).

We also considered comparison of our sequence to existing GenBank *H. influenzae* Rd sequences as a method for evaluating sequence accuracy as reported for yeast chromosome VIII (32). Unlike yeast, only a limited number of *H. influenzae* sequences are in GenBank (38 *H. influenzae* Rd accessions) and these are not necessarily of high

accuracy. The results of such a comparison show that our sequence is 99.67 percent identical overall to those GenBank sequences annotated as *H. influenzae* Rd. Two problems were apparent with this type of comparison. Sequences could differ because of strain variation, which is poorly annotated in the GenBank entries. It is also difficult to evaluate the significance of differences as the accuracy of the GenBank entries was impossible to assess. We compared GenBank accession M86702 (*strA* resistance gene) to our sequence and found the identity to be 94.7 percent over 545 bp. There are 24 single base pair mismatches relative to our sequence as well as an insertion and a deletion. Comparison of our sequence to GenBank accession L23824 (adenylate cyclase) shows a 99.7 percent match over 2960 bp. There are nine single base pair mismatches and one insertion. In this case the mismatches all fall in the noncoding flanking regions. While we cannot speak to the accuracy of these GenBank sequences, we are very confident of our sequences in these regions because of the 3 \times to 9 \times coverage with high-quality sequence data. Thus, a comparison of our sequence to sequences in GenBank annotated as *H. influenzae* Rd is not a meaningful way to evaluate the accuracy of the sequence.

Although it is extremely difficult to assess sequence accuracy, we wanted to provide an approximation of accuracy based on frequency of shifts in open reading frames, unresolved ambiguities, overall quality of raw data, and fold coverage. We estimate our error rate to be between 1 base in 5000 and 1 base in 10,000.

We also attempted to estimate the cost of the complete sequencing of the genome. Reagent and labor costs for construction of small insert and λ libraries, template preparation and sequencing, gap closure, sequence confirmation, annotation, and preparation for publication were summed and divided by the genome length. Sequencing projects that require up front mapping should include the cost of construction of the clone maps for sequencing. Not included were costs associated with development of technology and software that will be used for future sequencing projects. The estimated direct cost was 48 cents per finished base pair. Because of the techniques developed during this project any future genomes of this size should cost less.

Data and software availability. The *H. influenzae* genome sequence has been deposited in the Genome Sequence DataBase (GSDB) with the accession number L42023 and is termed version 1.0. The nucleotide sequence and peptide translation of each predicted coding region with identified start and stop codons have also been accessioned

by GSDB. We consider annotation, accuracy checking, and error resolution to be ongoing tasks. As outlined above, there are predicted coding regions with potential frameshift errors in the sequence. As these are resolved, they will be deposited with GSDB. We also expect the annotation of the sequence to increase over time and be updated in GSDB.

Additional data are available on our World Wide Web site (<http://www.tigr.org>). An expanded version of Table 3 has links to the database accessions that were used to identify the predicted coding regions, additional sequence similarity data, and coordinates of the predicted coding regions. The alignments between the predicted coding regions and the database sequences are also available. The data can also be queried by gene identification number, putative identification, matching accession, and role. The entire sequence and the sequences of all predicted coding regions and their translations, including those having frameshifts, are also available. This Web site will be maintained as an up-to-date source of *H. influenzae* genome sequence data, and we encourage the scientific community to forward their results for inclusion (with proper attribution) at this site.

The software developed at TIGR that is described in the article is still under development. However, TIGR will work with other genome centers to make its software available upon request.

Genome analysis. We have attempted to predict all of the coding regions and identify genes, transfer RNAs (tRNAs) and rRNAs, as well as other features of the DNA sequence (such as repeats, regulatory sites, replication origin sites, and nucleotide composition), with the realization that biochemical and biological conformation of many of these will be an ongoing task. We include a description of some of the most obvious sequence features.

The *H. influenzae* Rd genome is a circular chromosome of 1,830,137 bp. The overall G+C nucleotide content is approximately 38 percent (A, 31 percent; C, 19 percent; G, 19 percent; T, 31 percent). The G+C content of the genome was examined with several window lengths to look for global structural features. With a window of 5000 bp, the G+C content is relatively even except for seven large regions rich in G+C and several regions rich in A+T (Fig. 1). The G+C-rich regions correspond to six rRNA operons and a cryptic mu-like prophage. Genes for several proteins similar to proteins encoded by bacteriophage mu are located at approximately position 1.56 to 1.59 Mbp of the genome. This area of the genome has a markedly higher G+C content than average for *H. influenzae* (~50 percent G+C compared to ~38 percent for

the rest of the genome).

The minimal origin of replication (*oriC*) in *E. coli* is a 245-bp region defined by three copies of a 13-bp repeat at one end (sites for initial DNA unwinding) and four copies of a 9-bp repeat (sites for DnaA binding, the first step in replication) at the other (33). An approximately 280-bp sequence containing structures similar to the three 13-bp and four 9-bp repeats defines the putative origin of replication in *H. influenzae* Rd. This region lies between sets of ribosomal operons *rmF*, *rmE*, *rmD* and *rmA*, *rmB*, *rmC*. These two groups of ribosomal operons are transcribed in opposite directions and the placement of the origin is consistent with their polarity for transcription. Termination of *E. coli* replication is marked by two 23-bp termination sequences located ~100 kb on either side of the midway point at which the two replication forks meet. Two potential termination sequences sharing a 10-bp core sequence with the *E. coli* termination sequence were identified in *H. influenzae*. These two regions are offset approximately 100 kb from a point approximately 180° opposite of the proposed origin of *H. influenzae* replication.

Six rRNA operons were identified. Each contains three subunits and a variable spacer region in the order: 16S subunit—spacer region—23S subunit—5S subunit. The subunit lengths are 1539, 2653, and 116 bp, respectively. The G+C content of the three ribosomal subunits (50 percent) is higher than that of the genome as a whole. The G+C content of the spacer region (38 percent) is consistent with the remainder of the genome. The nucleotide sequence of the three rRNA subunits is completely identical in all six ribosomal operons. The rRNA operons can be grouped into two classes based on the spacer region between the 16S and 23S sequences. The shorter of the two spacer regions is 478 bp (*rrmB*, *rrmE*, and *rrmF*) and contains the gene for tRNA^{Glu}. The longer spacer is 723 bp (*rrmA*, *rrmC*, and *rrmD*) and contains the genes for tRNA^{Ile} and tRNA^{Ala}. The two sets of spacer regions are also completely identical across each group of three operons. Other tRNA genes are present at the 16S and 5S ends of two of the rRNA operons. The genes for tRNA^{Arg}, tRNA^{His}, and tRNA^{Pro} are located at the 16S end of *rrmE* while the genes for tRNA^{Trp} and tRNA^{Asp} are located at the 5S end of *rrmA*.

The predicted coding regions were initially defined by evaluating their coding potential with the program GENEMARK (34) based on codon frequency matrices derived from 122 *H. influenzae* coding sequences in GenBank. The predicted coding region sequences (plus 300 bp of flanking sequence) were used in searches against a database of nonredundant bacterial proteins

(NRBP) created specifically for the annotation. Redundancy was removed from NRBP at two stages. All DNA coding sequences were extracted from GenBank (release 85), and sequences from the same species were searched against each other. Sequences having more than 97 percent identity over regions longer than 100 nucleotides were combined. In addition, the sequences were translated and used in protein comparisons with all sequences in Swiss-Prot (release 30). Sequences belonging to the same species and having more than 98 percent similarity over 33 amino acids were combined. NRBP is composed of 21,445 sequences extracted from 23,751 GenBank sequences and 11,183 Swiss-Prot sequences from 1099 different species.

A total of 1743 predicted coding regions was identified. Searches of the predicted coding regions for *H. influenzae* were performed against NRBP with BLAZE (35) run on a Maspar MP-2 massively parallel computer with 4096 microprocessors. BLAZE translates the query DNA sequence in the three plus-strand reading frames and identifies the protein sequences that match the query. The protein-protein matches were aligned with PRAZE, a modified Smith-Waterman (23) algorithm. In cases where insertions or deletions in the DNA sequence produced a potential frameshift, the alignment algorithm started with protein regions of maximum similarity and extended the alignment to the same database match in alternative frames by means of the 300-bp flanking region. Unidentified predicted coding regions and the remaining intergenic sequences were searched against a dataset of all available peptide sequences from Swiss-Prot, the Protein Information Resource (PIR), and GenBank. Identification of operon structures is expected to be facilitated by experimental determination of promoter and termination sites.

Each putatively identified *H. influenzae* gene was assigned to one of 102 biological role categories adapted from Riley (36). Assignments were made by linking the protein sequence of the predicted coding regions with the Swiss-Prot sequences in the Riley database. Of the 1743 predicted coding regions, 736 have no role assignment. Of these, no database match was found for 389, while 347 matched "hypothetical proteins" in the database. Role assignments were made for 1007 of the predicted coding regions. Each of the 102 role categories was grouped into one of 14 broader role categories (Table 2). A compilation of all the predicted coding regions, their identifiers, a three-letter gene identifier, and percent similarity are presented in Table 3 (fold-out). An annotated complete genome map of *H. influenzae* Rd is presented in Fig. 2 (fold-out). The map places each predicted

coding region on the *H. influenzae* chromosome, indicates its direction of transcription and color codes its role assignment. Role assignments are also represented in Fig. 1.

A survey of the genes and their chromosomal organization in *H. influenzae* Rd makes possible a description of the metabolic processes *H. influenzae* requires for survival as a free-living organism, the nutritional requirements for its growth in the laboratory, and the characteristics that make it different from other organisms specifically as they relate to its pathogenicity and virulence. The genome would be expected to have complete complements of certain classes of genes known to be essential for life. For example, there is a one-to-one correspondence of published *E. coli* ribosomal protein sequences to potential homologs in the *H. influenzae* database. Likewise, as shown in Table 3, an aminoacyl tRNA synthetase is present in the genome for each amino acid. Finally, the location of tRNA genes was mapped onto the genome. There are 54 identified tRNA genes, including representatives of all 20 amino acids.

In order to survive as a free-living organism, *H. influenzae* must produce energy in the form of ATP via fermentation or electron transport. As a facultative anaerobe, *H. influenzae* Rd is known to ferment glucose, fructose, galactose, ribose, xylose, and fucose (37). As indicated by the genes identified in Table 3, transport systems are available for the uptake of these sugars by the phosphoenolpyruvate-phosphotransferase system (PTS), and by non-PTS mechanisms. Genes that specify the common phosphate-carriers enzyme I and Hpr (*ptsI* and *ptsH*) of the PTS system were identified as well as the glucose-specific *crr* gene. We have not, however, identified the gene-encoding, membrane-bound, glucose-specific enzyme II. The latter enzyme is required for transport of glucose by the PTS system. A complete PTS system for fructose was identified.

Genes encoding the complete glycolytic pathway and for the production of fermentative end products were identified. Also identified were genes encoding functional anaerobic electron transport systems that depend on inorganic electron acceptors such as nitrates, nitrites, and dimethyl sulfoxide. Genes encoding three enzymes of the tricarboxylic acid (TCA) cycle appear to be absent from the genome. Citrate synthase, isocitrate dehydrogenase, and aconitase were not found by searching the predicted coding regions or by using the *E. coli* enzymes as peptide queries against the entire genome in translation. This provides an explanation for the large amount of glutamate (1 g/liter) that is required in defined culture media (38). Glutamate can be directed into the TCA cycle by conversion to α -ketoglutarate by glutamate dehydrogenase. In the absence of a complete TCA cycle, glutamate presumably serves as the source of carbon for biosynthesis of amino acids from precursors that branch from the TCA cycle. Functional electron transport systems that depend on oxygen as a terminal electron acceptor are available for the production of adenosine triphosphate.

Previously unanswered questions regarding pathogenicity and virulence can be addressed by examining certain classes of genes such as adhesins and the lipo-oligosaccharide biogenesis genes. Moxon and co-workers (31) have obtained evidence that a number of these virulence-related genes contain tandem tetramer repeats that undergo frequent addition and deletion of one or more repeat units during replication such that the reading frame of the gene is changed and its expression thereby altered. It is now possible, by means of the complete genome sequence, to locate all such tandem repeat tracts (Fig. 2) and to begin to determine their roles in phase variation of such potential virulence genes.

Haemophilus influenzae Rd has a highly efficient, DNA transformation system. The DNA uptake sequence site, 5' AAGTGC-GGT, present in multiple copies in the genome, is necessary for efficient DNA uptake (39). It is now possible to locate all of these sites and describe their distribution with respect to genic and intergenic regions (40). Fifteen genes involved in transformation have already been described and sequenced (41). Six of the genes, *comA* to *comF*, comprise an operon that is under positive control by a 22-bp, palindromic, competence regulatory element (CRE) located approximately one helix turn upstream of the promoter. It is now feasible to locate additional copies of CRE in the genome and discover potential transformation genes under CRE control (42). In addition, other global regulatory elements may be discovered with an ease not previously possible.

One well-described system for gene regulation in bacteria is the "two-component" system composed of a sensor molecule that detects an environmental signal and a regulator molecule that is phosphorylated by the activated form of the sensor. The regulator protein is generally a transcription factor that, when activated by the sensor, turns on or off expression of a specific set of genes. It has been estimated that *E. coli* harbors 40 sensor-regulator pairs (43). The *H. influenzae* genome was searched with representative proteins from each family of sensor and regulator proteins with TBLASTN and TFASTA. Four sensor and five regulator proteins were identified with similarity to proteins from other species (Table 4). There appears to be a corresponding sensor for each regulator protein except CpxR. Searches with the CpxA protein from *E. coli* identified three of the four sensors listed in Table 4, but no additional significant matches were found. It is possible that the sequence similarity is low enough to be undetectable with TFASTA. All of the regulator proteins present fall into the OmpR subclass (43). No representatives of the NtrC class of regulators were found. This class of proteins interacts directly with the sigma-54 subunit of RNA polymerase, which is absent from *H. influenzae*, and which plays a major role in the regulation of a large number of operons in *E. coli* and other enterobacteria. The absence of the Ntr network in *H. influenzae* suggests significant differences in the regulatory processes between these two groups of organisms.

Some of the most interesting questions that can be answered by a complete genome sequence relate to the genes or pathways that are absent. The nonpathogenic *H. influenzae* Rd strain varies significantly from the pathogenic serotype b strains. Many of the differences between these two strains appear in factors affecting infectivity. For example, we have found that the eight genes that make up the fimbrial gene cluster (44) involved in adhesion of bacteria to host cells are absent in the Rd strain. The *pepN* and *purE* genes, which flank the fimbrial cluster in *H. influenzae* type b strains,

Table 4. Two-component systems in *H. influenzae* Rd. ID, identity; Sim, similarity.

Identification number	Location	Best match*	Id (%)	Sim (%)	Length (bp)
<i>Sensors</i>					
HI0220	239,378	<i>arcB</i>	39.5	63.9	200
HI0267	299,541	<i>narQ</i>	38.1	68.0	562
HI1707	1,781,143	<i>basS</i>	27.7	51.5	250
HI1378	1,475,017	<i>phoR</i>	38.1	61.6	280
<i>Regulators</i>					
HI0726	777,934	<i>narP</i>	59.3	77.0	209
HI0837	887,011	<i>cpxR</i>	51.9	73.0	229
HI0884	936,624	<i>arcA</i>	77.2	87.8	236
HI1379	1,475,502	<i>phoB</i>	52.9	71.4	228
HI1708	1,781,799	<i>basR</i>	43.5	59.3	219

*In all cases, the best match was to a gene of *E. coli*.

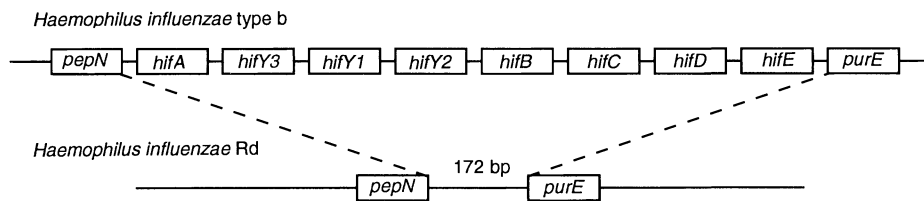


Fig. 3. A comparison of the region of the *H. influenzae* chromosome containing the eight genes of the fimbrial gene cluster present in *H. influenzae* type b and the same region in *H. influenzae* Rd. The region is flanked by *pepN* and *purE* in both organisms. However, in the noninfectious Rd strain the eight genes of the fimbrial gene cluster have been excised. A 172-bp spacer region is located in this region in the Rd strain and continues to be flanked by the *pepN* and *purE* genes.

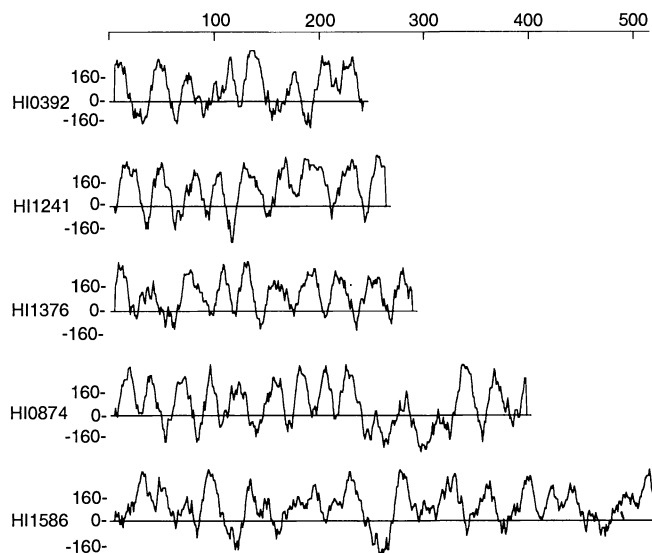
are adjacent to one another in the Rd strain (Fig. 3), suggesting that the entire fimbrial cluster was excised.

On a broader level, we determined which *E. coli* proteins are not in *H. influenzae* by taking advantage of a nonredundant set of protein-coding genes from *E. coli*, namely the University of Wisconsin Genome Project contigs in GenBank: 1216 predicted protein sequences from GenBank accessions D10483, L10328, U00006, U00039, U14003, and U18997 (45). The minimum threshold for matches was set so that even weak matches would be scored as positive, thereby giving a minimal estimate of the *E. coli* genes not present in *H. influenzae*. We used TBLASTN to search each of the *E. coli* proteins against the complete genome. All BLAST scores greater than 100 were considered matches. Altogether 627 *E. coli* proteins matched at least one region of the *H. influenzae* genome and 589 proteins did not. The 589 nonmatching proteins were examined and found to contain a disproportionate number of hypothetical proteins from *E. coli*. Sixty-eight percent of the identified *E. coli* proteins were matched by an *H. influenzae* sequence whereas only 38 percent of the hypothetical proteins were matched. Proteins are anno-

tated as hypothetical on the basis of a lack of matches with any other known proteins (45). At least two potential explanations can be offered for the overrepresentation of hypothetical proteins among those without matches: (i) some of the hypothetical proteins are not, in fact, translated (at least in the annotated frame), or (ii) these are *E. coli*-specific proteins that are unlikely to be found in any species except those most closely related to *E. coli*, for example, *Salmonella typhimurium*.

A total of 389 predicted coding regions did not display significant similarity with a six-frame translation of GenBank release 87. These unidentified coding regions were compared to one another with FASTA. Two previously unidentified gene families were identified. Two predicted coding regions without database matches (HI0589 and HI0850) share 75 percent identity over almost their entire lengths (139 and 143 amino acid residues respectively). A second pair of predicted coding regions (HI1555 and HI1548) encode proteins that share 30 percent identity over almost their entire lengths (394 and 417 amino acids respectively). These similarities suggest that there may be previously unidentified gene families present in these regions.

Fig. 4. Hydrophobicity analysis of five potential channel proteins. The amino acid sequences of five predicted coding regions that do not display similarity with known peptide sequences (GenBank release 87), each exhibit multiple hydrophobic domains that are characteristic of channel-forming proteins. The predicted coding region sequences were analyzed by the Kyte-Doolittle algorithm (46) (with a range of 11 residues) with the GENWORKS software package (Intelligenetics).



Another analysis that can be applied to the unidentified coding regions is hydropathy analysis, which indicates the patterns of potential membrane-spanning domains that are often conserved between members of receptor and transporter gene families, even in the absence of significant amino acid identity. The five best examples of unidentified predicted coding regions that display potential transmembrane domains with a periodic pattern that is characteristic of membrane-bound channel proteins are shown in Fig. 4. Such information can be used to focus on specific aspects of cellular function that are affected by targeted deletion or mutation of these genes.

We have learned some important lessons concerning overall strategy from the *H. influenzae* sequencing project that should reduce the effort required for future bacterial genome sequencing projects. For example, the small insert library and the large insert library should be constructed and end-sequenced concurrently. It is essential that the sequence fragments used for the assembly are of the highest quality. The sequences should be rigorously checked for vector contamination. Although it is important that sequence read lengths be long enough to span most small repeats, they must also be highly accurate. Our raw sequence data contained on average less than 1.5 percent uncertainties. The use of high quality individual sequence fragments and a rigorous assembly algorithm essentially eliminated difficulty with achieving closure. The success of whole genome shotgun sequencing offers the potential to accelerate research in a number of areas. Comparative genomics could be advanced by the availability of an increased number of complete genomes from a variety of prokaryotes and eukaryotes. Knowledge of the complete genomes of pathogenic organisms could lead to new vaccines. Information obtained from the genomes of particular organisms could have industrial applications. Finally, this strategy has potential to facilitate the sequencing of the human genome.

REFERENCES AND NOTES

1. F. Sanger *et al.*, *Nature* **246**, 687 (1977); F. Sanger, A. R. Coulson, G. F. Hong, D. F. Hill, G. B. Petersen, *J. Mol. Biol.* **162**, 729 (1982).
2. A. T. Bankier *et al.*, *DNA Seq.* **2**, 1 (1991).
3. S. J. Goebel *et al.*, *Virology* **179**, 247 (1990).
4. K. Oda *et al.*, *J. Mol. Biol.* **223**, 1 (1992); K. Ohyama *et al.*, *Nature* **322**, 572 (1986).
5. R. F. Massung *et al.*, *Nature* **366**, 748 (1993).
6. D. L. Hartl and M. J. Palazzolo, *Genome Research in Molecular Medicine and Virology*, K. W. Adolph, Ed. (Academic Press, Orlando, FL, 1993), pp. 115–129.
7. H. J. Sofia *et al.*, *Nucleic Acids Res.* **22**, 2576 (1994).
8. J. Levy, *Yeast* **10**, 1689 (1994).
9. P. Glaser *et al.*, *Mol. Microbiol.* **10**, 371 (1993).
10. J. Sulston *et al.*, *Nature* **356**, 37 (1992).
11. W. F. Bodmer, *Rev. Invest. Clin.* (suppl., pp. 3–5) (1994).
12. M. D. Adams, C. Fields, J. C. Venter, Eds. *Automat-*

ed DNA Sequencing and Analysis (Academic Press, San Diego, CA, 1994).

13. M. D. Adams *et al.*, *Science* **252**, 1651 (1991); M. D. Adams *et al.*, *Nature* **355**, 632 (1992); M. D. Adams *et al.*, *ibid.*, in press.
14. E. S. Lander and M. S. Waterman, *Genomics* **2**, 231 (1988).
15. *Haemophilus influenzae* Rd KW20 DNA was prepared by extraction with phenol. A mixture (3.3 ml) containing 600 µg of DNA, 300 mM sodium acetate, 10 mM tris-HCl, 1 mM Na-EDTA, and 30 percent glycerol was sonicated (Branson Model 450 Sonicator) at the lowest energy setting for 1 minute at 0°C with a 3-mm probe. The DNA was precipitated in ethanol and redissolved in 500 µl of tris-EDTA (TE) buffer to create blunt ends; a 100-µl portion was digested for 10 minutes at 30°C in 200 µl of BAL 31 buffer with 5 units of BAL 31 nuclease (New England BioLabs). The DNA was extracted with phenol, precipitated in ethanol, redissolved in 100 µl of TE buffer, and fractionated on a 1.0 percent low melting agarose gel. A fraction (1.6 to 2.0 kb) was excised, extracted with phenol, and redissolved in 20 µl of TE buffer. A two-step ligation procedure was used to produce a plasmid library in which 97 percent of the recombinants contained inserts, of which >99 percent were single inserts. The first ligation mixture (50 µl) contained 2 µg of DNA fragments, 2 µg of Sma I + bacterial alkaline phosphatase pUC18 DNA (Pharmacia), and 10 units of T4 ligase (Gibco/BRL), and incubation was at 14°C for 4 hours. After extraction with phenol and ethanol precipitation, the DNA was dissolved in 20 µl of TE buffer and separated by electrophoresis on a 1.0 percent low melting agarose gel. A ladder of ethidium bromide-stained linearized DNA bands, identified by size as insert (i), vector (v), v+i, v+2i, v+3i, and so on, was visualized by 360-nm ultraviolet light, and the v+i DNA was excised and recovered in 20 µl of TE. The v+i DNA was blunt-ended by T4 polymerase treatment for 5 minutes at 37°C in a reaction mixture (50 µl) containing the linearized v+i fragments four deoxynucleotide triphosphates (dNTPs) (500 µM each) and 9 units of T4 polymerase (New England BioLabs) under buffer conditions recommended by the supplier. After phenol extraction and ethanol precipitation, the repaired v+i linear pieces were dissolved in 20 µl of TE. The final ligation to produce circles was carried out in a 50-µl reaction containing 5 µl of v+i DNA and 5 units of T4 ligase at 14°C overnight. The reaction mixture was heated for 10 minutes at 70°C and stored at -20°C.
16. A 100-µl portion of Epicurian Coli SURE 2 Super-competent Cells (Stratagene 200152) was thawed on ice and transferred to a chilled Falcon 2059 tube on ice. A 1.7-µl volume of 1.42 M β-mercaptoethanol was added to the cells to a final concentration of 25 mM. Cells were incubated on ice for 10 minutes. A 1-µl sample of the final ligation mix was added to the cells and incubated on ice for 30 minutes. The cells were heat-treated for 30 seconds at 42°C and placed back on ice for 2 minutes. The outgrowth period in liquid culture was omitted to minimize the preferential growth of any given transformed cell. Instead, the transformed cells were plated directly on a nutrient rich SOB plate containing a 5-ml bottom layer of SOB agar (1.5 percent SOB agar consisted of 20 g of tryptone, 5 g of yeast extract, 0.5 g of NaCl, and 1.5 percent Difco agar/liter). The 5-ml bottom layer was supplemented with 0.4 ml of ampicillin (50 mg/ml) per 100 ml of SOB agar. The 15-ml top layer of SOB agar was supplemented with 1 ml of X-gal (2 percent), 1 ml of MgCl₂ (1 M), and 1 ml of MgSO₄ (1 M) per 100 ml of SOB agar. The 15-ml top layer was poured just before plating. Our titer was approximately 100 colonies per 10-µl aliquot of transformation.
17. K. W. Wilcox and H. O. Smith, *J. Bact.* **122**, 443 (1975).
18. A. Greener, *Strategies* **3**, 5 (1990).
19. T. R. Utterback *et al.*, in preparation.
20. For the unamplified λ library, *H. influenzae* Rd KW20 DNA (>100 kb) was partially digested in a reaction mixture (200 µl) containing 50 µg of DNA, 1 × Sau3A I buffer, and 20 units of Sau3A I for 6 minutes at 23°C. The digested DNA was extracted with phenol and fractionated on a 0.5 percent low melting agarose gel at 2 V/cm for 7 hours. Fragments from 15 to 25 kb were excised and recovered in a final volume of 6 µl. We used 1 µl of fragments with 1 µl of DASHII vector (Stratagene) in the recommended ligation reaction. One microliter of the ligation mixture was used per packaging reaction as recommended in the protocol with the Gigapack II XL Packaging Extract (Stratagene, 227711). Phage were plated directly without amplification from the packaging mixture (after dilution with 500 µl of recommended SM buffer and treatment with chloroform). [SM buffer contains (per liter) 5.8 g of NaCl, 2 g of MgSO₄ · H₂O, 50 ml of 1 M tris-HCl, pH 7.5, and 5 ml of a 2 percent solution of gelatin.] The yield was about 2.5 × 10³ plaque-forming units (PFU) per microliter. The amplified library was prepared essentially as above except the λ GEM-12 vector was used. After packaging, about 3.5 × 10⁴ PFU were plated on the restrictive NM539 host. The lysate was harvested in 2 ml of SM buffer and stored frozen in 7 percent dimethyl sulfoxide. The phage titer was approximately 1 × 10⁹ PFU/ml.
21. M. D. Adams, *et al.*, *Nature* **368**, 474 (1994).
22. A. R. Kerlavage *et al.*, *Proceedings of the Twenty-Sixth Annual Hawaii International Conference on System Science* (IEEE Computer Society Press, Washington, DC, 1993), p. 585; A. R. Kerlavage *et al.*, *IEEE Computers in Medicine and Biology* (IEEE, Computer Society Press, Washington, DC, in press).
23. M. S. Waterman, *Methods Enzymol.* **164**, 765 (1988).
24. W. Pearson and D. Lipman, *Proc. Natl. Acad. Sci. U.S.A.* **85**, 2444 (1988).
25. Oligonucleotides were labeled by combining 50 pmol of each 20-mer and 250 mCi of [³²P] adenosine triphosphate and T4 polynucleotide kinase. The labeled oligonucleotides were purified with Sephadex G-25 superfine (Pharmacia). A portion containing 10⁷ counts per minute of each was used in a Southern hybridization analysis of *H. influenzae* Rd chromosomal DNA digested with one frequently cleaving endonuclease (Ase I) and five less-frequent ones (Bgl II, Eco RI, Pst I, Xba I, and Pvu II). The DNA from each digest was fractionated on a 0.7 percent agarose gel and transferred to nylon (Nytran Plus) membranes (Schleicher & Schuell). Hybridization was carried out for 16 hours at 40°C. To remove nonspecific signals, we sequentially washed each blot at room temperature with increasingly stringent conditions up to 0.1 × saline sodium citrate and 0.5 percent SDS. Blots were exposed to a PhosphorImager cassette (Molecular Dynamics) for several hours; hybridization patterns were compared visually.
26. S. Altschul *et al.*, *J. Mol. Biol.* **215**, 403 (1990).
27. E. F. Kirkness *et al.*, *Genomics* **10**, 985 (1991).
28. Standard amplification by polymerase chain reaction (PCR) was performed in the following manner. Each reaction (57 µl) contained a 37-µl mixture of 16.5 µl of H₂O, 3 µl of 25 mM MgCl₂, 8 µl of a dNTP mix (1.25 mM each dNTP), 4.5 µl of 10 × PCR core buffer II (Perkin-Elmer N808-0009), and 25 ng of *H. influenzae* Rd KW20 genomic DNA. The appropriate two primers (4 µl, 3.2 pmol/µl) were added to each reaction. A preliminary incubation (hotstart) was performed at 95°C for 5 minutes followed by a 75°C hold. During the holding period, Amplitaq DNA polymerase (Perkin-Elmer N801-0060, 0.3 µl in 4.3 µl of H₂O, 0.5 µl of 10 × PCR core buffer II) was added to each reaction. The PCR profile was 25 cycles of 94°C for 45 seconds, then denature; 55°C for 1 minute, then anneal; 72°C for 3 minutes, then extension. All reactions were performed in a 96-well format on a Perkin-Elmer GeneAmp PCR System 9600. Long-range PCR was performed as follows: Each reaction contained a 35.2-µl mixture of 12.0 µl of H₂O, 2.2 µl of 25 mM magnesium acetate, 4 µl of a dNTP mixture (200 µM final concentration), 12.0 µl of 3.3 × PCR buffer, and 25 ng of *H. influenzae* Rd KW20 genomic DNA. The appropriate two primers (5 µl, 3.2 pmol/µl) were added to each reaction. A preliminary incubation (hot start) was performed at 94°C for 1 minute. Then *r7th* polymerase (Perkin-Elmer N808-0180) (4 units per reaction) in 2.8 µl of 3.3 × PCR buffer II was added to each reaction. The PCR profile was 18 cycles of 94°C for 15 seconds, denature; 62°C for 8 minutes, anneal and extend followed by 12 cycles 94°C for 15 seconds, denature; 62°C for 8 minutes (increase 15 per cycle), anneal and extend; and 72°C for 10 minutes, final extension. All reactions were done in a 96-well format on a Perkin-Elmer GeneAmp PCR System 9600.
29. J. J. Lee, H. O. Smith, R. R. Redfield, *J. Bacteriol.* **171**, 3016 (1989).
30. J. M. Claverie, *J. Mol. Biol.* **234**, 1140 (1993).
31. J. N. Weiser *et al.*, *Cell* **59**, 657 (1989).
32. M. Johnston *et al.*, *Science* **265**, 2077 (1994).
33. B. Lewin, Ed., *Genes V* (Oxford Univ. Press, New York, 1994), chaps. 18 and 19.
34. M. Borodovsky and J. McIninch, *Comp. Chem.* **17**, 123 (1993). In the GeneMark program second-order phased Markov chain models were used; it was trained on 188,572 bp of protein coding sequence and 33,118 bp of noncoding sequence as annotated in GenBank *H. influenzae* entries. It was shown that the second-order program is the most accurate given the size of the training set. The accuracy level was assessed by a cross-validation procedure with a set of 96-bp nonoverlapping fragments derived from the same sets of sequences. With the use of a threshold of 0.5, coding fragments were identified correctly in 91.2 percent of the cases; noncoding fragments were identified correctly in 93.3 percent of the cases.
35. D. Brutlag *et al.*, *ibid.*, p. 203. The BLOSUM 60-amino acid substitution matrix was used in all protein-protein comparisons [S. Henikoff and J. G. Henikoff, *Proc. Natl. Acad. Sci. U.S.A.* **89**, 10915 (1992)].
36. M. Riley, *Microbiol. Rev.* **57**, 862 (1993).
37. I. R. Dorocicz *et al.*, *J. Bacteriol.* **175**, 7142 (1993); B. Dougherty, unpublished results.
38. R. D. Klein and G. H. Luginbuhl, *J. Gen. Microbiol.* **113**, 409 (1979).
39. D. B. Danner *et al.*, *Gene* **11**, 311 (1980); D. B. Danner *et al.*, *Proc. Natl. Acad. Sci. U.S.A.* **79**, 2393 (1982); M. E. Kahn and H. O. Smith, *J. Membr. Biol.* **138**, 155 (1984).
40. H. O. Smith *et al.*, *Science* **269**, 538 (1995).
41. R. R. Redfield, *J. Bacteriol.* **173**, 5612 (1991); M. S. Chandler, *Proc. Natl. Acad. Sci. U.S.A.* **89**, 1616 (1992); R. Barouki and H. O. Smith, *J. Bacteriol.* **163**, 629 (1985); J.-F. Tomb, H. El-Haji, H. O. Smith, *Gene* **104**, 1 (1991); J.-F. Tomb, *Proc. Natl. Acad. Sci. U.S.A.* **89**, 10252 (1992).
42. J.-F. Tomb, unpublished results.
43. L. M. Albright, E. Huala, F. M. Ausubel, *Annu. Rev. Genet.* **23**, 311 (1989); J. S. Parkinson and E. C. Kofoid, *Am. Rev. Genet.* **26**, 71 (1992).
44. M. S. vanHam, L. vanAlphen, F. R. Mooi, J. P. Van-der-Pluijm, *Mol. Microbiol.* **13**, 673 (1994).
45. T. Yura *et al.*, *Nucleic Acids Res.* **20**, 3305 (1992); V. Burland *et al.*, *Genomics* **16**, 551 (1993).
46. J. Klyte and R. F. Doolittle, *J. Mol. Biol.* **157**, 105 (1982).
47. Supported in part by a core grant from Human Genome Sciences and an American Cancer Society grant (NP-838C) (to H.O.S.). Reagents for sequencing reactions and the synthesis of the oligonucleotides were a gift from the Applied Biosystems Division of Perkin-Elmer. We thank T. Burcham of Applied Biosystems for his contribution in the development of the TIGR EDITOR software; M. Riley, Marine Biological Laboratory, Woods Hole, for making her *E. coli* database available; M. Borodovsky and W. Hayes, School of Biology, Georgia Institute of Technology for providing and tuning the GeneMark software for use with *H. influenzae*; and J. Kelley, T. Dixon, and V. Sapiro for their excellent computer system support. H.O.S. is an American Cancer Society research professor.

16 May 1995; accepted 28 June 1995